NAVAL POSTGRADUATE SCHOOL
Monterey, California

THESIS

ACOUSTIC PROPAGATION
IN THE SOMALI BASIN

by

James Samuel Hanna

December 1980

Thesis Advisor: R. H. Bourke

REPORT DOCUMENTATION PAGE

READ INSTRUCTIONS BEFORE COMPLETING FORM

1. REPORT NUMBER
2. GOVT ACCESSION NO.
3. RECIPIENT'S CATALOG NUMBER

4. TITLE (and Subtitle)
Acoustic Propagation in the Somali Basin

5. TYPE OF REPORT & PERIOD COVERED
Master's Thesis; December 1980

6. PERFORMING ORG. REPORT NUMBER

7. AUTHOR(s)
James Samuel Hanna

8. CONTRACT OR GRANT NUMBER(s)

9. PERFORMING ORGANIZATION NAME AND ADDRESS
Naval Postgraduate School
Monterey, California 93940

10. PROGRAM ELEMENT, PROJECT, TASK AREA & WORK UNIT NUMBERS

11. CONTROLLING OFFICE NAME AND ADDRESS
Naval Postgraduate School
Monterey, California 93940

12. REPORT DATE
December 1980

13. NUMBER OF PAGES
93

14. MONITORING AGENCY NAME & ADDRESS(if different from Controlling Office)

15. SECURITY CLASS. (of this report)
Unclassified

15a. DECLASSIFICATION/DOWNGRADING SCHEDULE

16. DISTRIBUTION STATEMENT (of this Report)
Approved for public release; distribution unlimited.

17. DISTRIBUTION STATEMENT (of the abstract entered in Block 20, if different from Report)

18. SUPPLEMENTARY NOTES

19. KEY WORDS (Continue on reverse side if necessary and identify by block number)
Somali Basin
Indian Ocean
ICAPS
Acoustic Propagation

20. ABSTRACT (Continue on reverse side if necessary and identify by block number)

Acoustic propagation in the Somali Basin region of the Indian Ocean was evaluated using the ICAPS program. Direct path range predictions were made for a towed array (100 Hz) at 100 m and a hull mounted sonar (2000 Hz) at 10 m sensing a signal generated by a source at 100 m. Predictions were based on climatological and recent observed data. These predictions were compared in order to ascertain the accuracy of

the ICAPS climatological prediction. In general, the ICAPS performed marginally well during the summer monsoon season with an average difference of 9% in predicted ranges at 100 Hz and 19% at 2000 Hz for a FOM of 100 or greater. However, predictions based on the winter season climatology were significantly in error with range predictions being over and under predicted by a factor of two.

Approved for public release; distribution unlimited.

Acoustic Propagation in the Somali Basin

by

James Samuel Hanna
Lieutenant, United States Navy
B.S., United States Naval Academy, 1975

Submitted in partial fulfillment of the
requirements for the degree of

MASTER OF SCIENCE IN OCEANOGRAPHY

from the

NAVAL POSTGRADUATE SCHOOL
December 1980

ABSTRACT

Acoustic propagation in the Somali Basin region of the Indian Ocean was evaluated using the ICAPS program. Direct path range predictions were made for a towed array (100 Hz) at 100 m and a hull mounted sonar (2000 Hz) at 10 m sensing a signal generated by a source at 100 m. Predictions were based on climatological and recent observed data. These predictions were compared in order to ascertain the accuracy of the ICAPS climatological prediction. In general, the ICAPS performed marginally well during the summer monsoon season with an average difference of 9 % in predicted ranges at 100 Hz and 19% at 2000 Hz for a FOM of 100 or greater. However, predictions based on the winter season climatology were significantly in error with range predictions being over and under predicted by a factor of two.

TABLE OF CONTENTS

LIST OF TABLES

LIST OF FIGURES

ACKNOWLEDGEMENTS

I wish to offer my sincere gratitude to Dr. R. H. Bourke for his tireless editing efforts and to Dr. C. N. K. Mooers for his continuing interest and guidance. I also wish to express my appreciation to my wife Linda for her great patience and understanding.

I. INTRODUCTION

Compared with the Atlantic and Pacific Oceans, the Indian Ocean is a little studied ocean. Recent efforts have been made to remedy this situation, but its remoteness from the U.S. causes research to be costly both in time and money. The U.S. Navy has recently stepped up its tempo of operations in response to the current instabilities in the Middle East. Carrier Battle Groups are now continuously deployed in the Indian Ocean. Because of the absence of a strong U.S. Navy presence in this area in the past, Battle Group crews are inexperienced in the nuances of the ocean aspects of the Indian Ocean which affect ASW operations.

A Battle Group transitting along the east African coast, through the Somali Basin and into the Arabian Sea, will have to depend heavily on surface ship acoustic sensors for the detection of hostile submarines. The tactical and strategic deployment of these ships depends in large measure on the expected performance of the various acoustic sensors. Assessment of sensor performance "in the field" is performed by Navy ASW units employing the Integrated Carrier ASW Prediction System (ICAPS). This computer system relies on either a recent sound speed profile (SSP) from the immediate area or a data bank of composite SSP's based on averaging archival temperature-salinity data from the region.

Historical temperature-salinity data from the Indian Ocean are quite sparse, limited in both time and space. Much of the data were acquired prior to the advent of continuously profiling instrumentation; hence, temperature-salinity inversions due to intermingling of water masses have been largely omitted. In addition, grouping of data to form spatial averages was necessarily performed without the aid of remote sensing techniques to identify water mass boundaries.

Because of the above inadequacies in the historical data, one can rightfully question the validity of acoustic performance assessments based on such data. It is the purpose of this study to evaluate acoustic performance based on the ICAPS climatological data files against that obtained in situ. Specifically, oceanographic data from recent cruises to the Somali Basin area, gathered during both the summer and winter monsoon seasons, will be used to evaluate the performance of two typical surface ship ASW sensors, a hull mounted sonar and a towed array. Each of these sensors is assumed to be listening for signals radiated by a transitting submarine, the former listening at 2000 Hz and the latter at 100 Hz.

II. OCEANOGRAPHY

A. GENERAL

This section is presented to provide the reader with an overview of the oceanography of the western Indian Ocean. A broad-scale view of the morphology, monsoonal climatology and ocean circulation is presented first. This is followed by a detailed analysis of the Somali Basin area based on several recent field experiments.

B. MORPHOLOGY

The Somali Basin (Figure 1) is bounded on the west by the continental rise and shelf of East Africa. The shelf in this area is narrow and poorly surveyed [Shepard, 1973]. In places along the straight coastline Shepard observed the lack of any shelf. This is suggestive of a fault origin of the coast. The shelf break occurs at an average depth of 140 m [Shepard, 1973]. The sediment on the east African shelf has had little study. Samples taken off Kenya and Somalia consisted of calcareous sands [Shepard, 1973]. The continental slope is generally less than 3° with a steeper slope off Somalia. The base of the slope was cited by Shepard as rarely deeper than 3000 m.

To the north lies the Arabian peninsula. The shelf here is also narrow and consists of rock and sand. In this area the shelf averages 38 km in width and the shelf break occurs

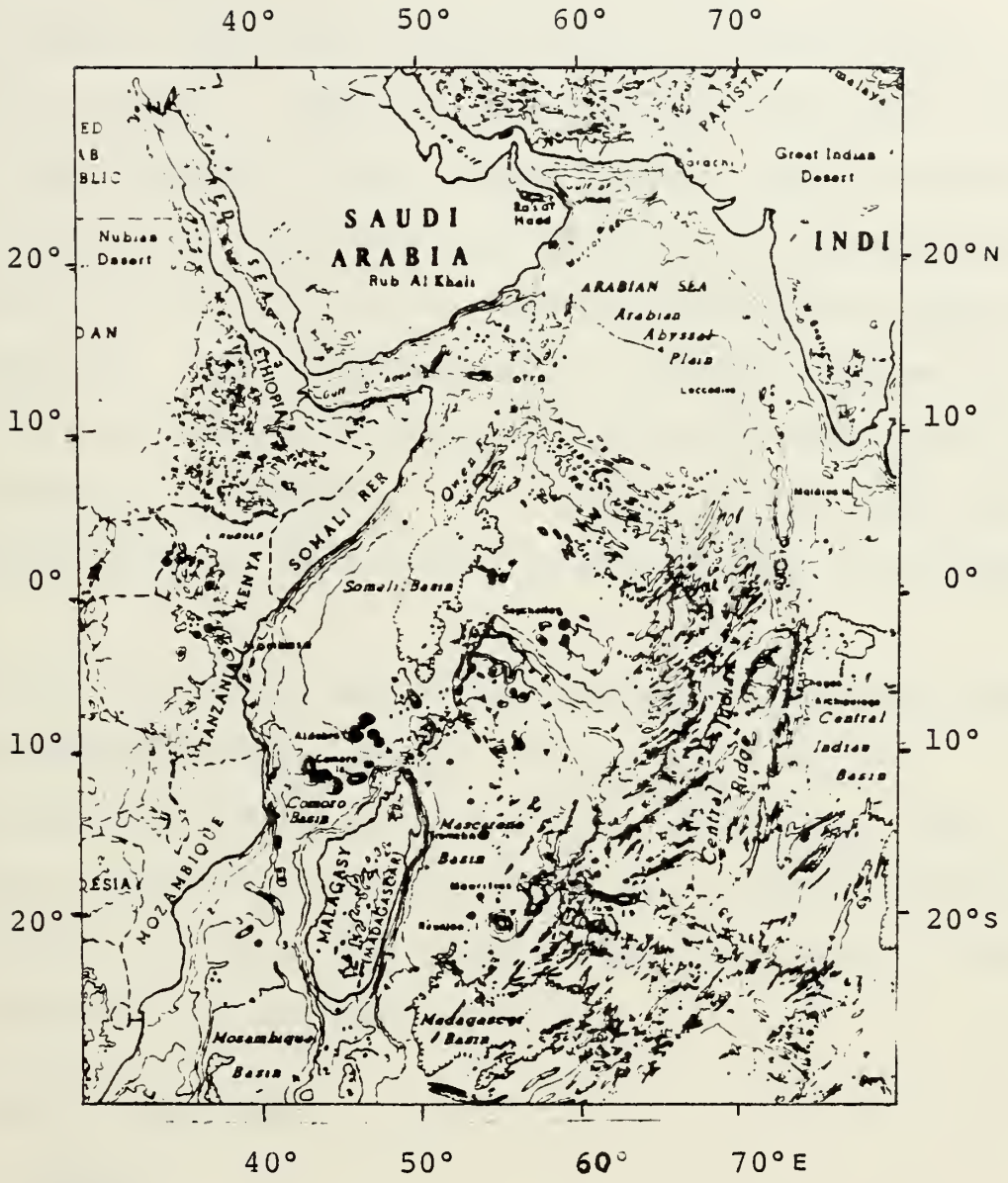

Figure 1. Important bathymetric features of the western Indian Ocean [from Colborn, 1976].

at an average depth of 75 m. At the entrance to the Red Sea, the channel consists of a rift valley [Shepard, 1973].

The Indian Ocean ridge system bounds the Somali Basin to the east (Figure 1). The Owen Fracture Zone marks the northern edge of the Carlsberg Ridge. Shepard [1973] states that the Owen Fracture Zone may extend for hundreds of kilometers to the north and south and may be connected with faults along the west Himalayas. The Carlsberg Ridge may have developed as a result of plate tectonics [Shephard, 1973] with spreading occurring northeast - southwest. The Carlsberg Ridge rises from the abyssal plain to 2500 m and contains breccia of ultramafic rocks.

South of the Somali Basin lies the Seychelles Bank composed of continental granite. Depths are less than 2000 m.

The Somali Basin is 5000 m in depth [Fairbridge, 1966]. The basin is covered with globegerina ooze. Sediment depth is in excess of 1 km at the western edge of the basin. The Somali Basin is regular and smooth.

C. MONSOON CLIMATOLOGY

1. General

The periodic reversal of the prevailing winds in the lower atmosphere, known as the monsoon, profoundly affects the circulation of the Indian Ocean. This monsoon (from the Arabic "marrsin," or season) is caused primarily by the differential heating of the Indian subcontinent and the Indian Ocean.

The existence of the monsoon regime was known at least as early as during the time of the Roman Empire when merchant vessels took advantage of the wind reversal to trade with India [Neumann and Pierson, 1966]. Edmund Halley proposed in 1628 that the monsoon was caused by differential heating. In 1921 Simpson supported Halley's hypothesis, but also emphasized the importance of topography (viz., the Himalayas) in anchoring the low pressure system over Pakistan in the summer [Cadet, 1979].

2. Northeast Monsoon

Figure 2 shows the pressure field during the northeast monsoon. During the winter season the land mass cools much more rapidly than does the ocean. A high pressure system forms over the cold land mass. This system causes a flow of air outward toward a low pressure system over the east African coast. This equatorial flow of air is the winter (northeast) monsoon. The winter monsoon is described as an easterly trade wind system much like the trade wind systems of the tropical Atlantic and Pacific because of the strong easterly component of the monsoon wind [Knox, 1980]. The winter monsoon is characterized by light, dry winds (1.6-3.3 m/sec) producing relatively calm seas (less than 1 m 55% of the time) (SP-68, HO-107).

3. Southwest Monsoon

Figure 3 depicts the pressure field during the summer season. As the summer approaches, the land mass of the subcontinent begins to warm. The high pressure system begins to

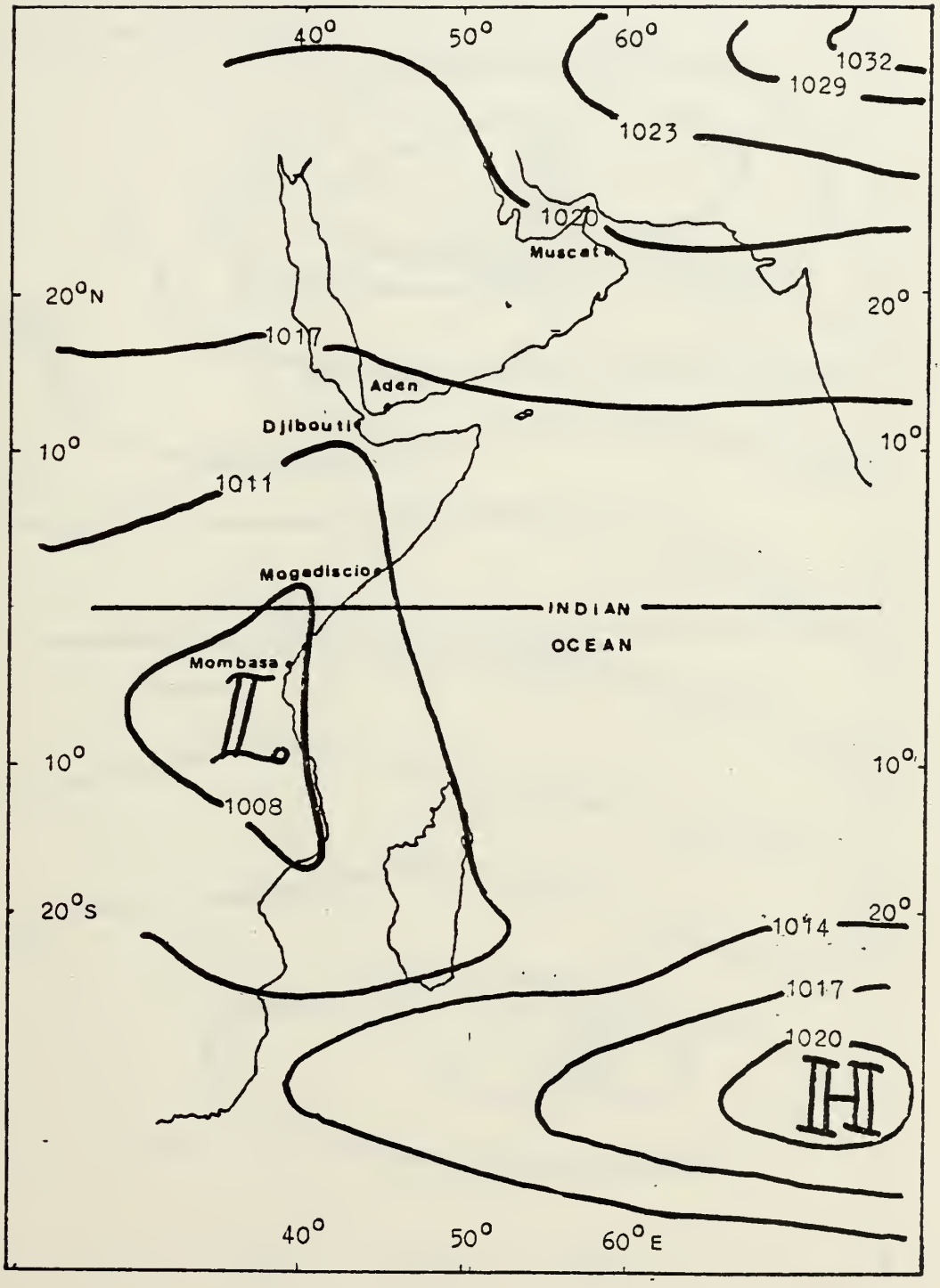

Figure 2. Pressure distribution during the winter monsoon [after Fairbridge, 1966].

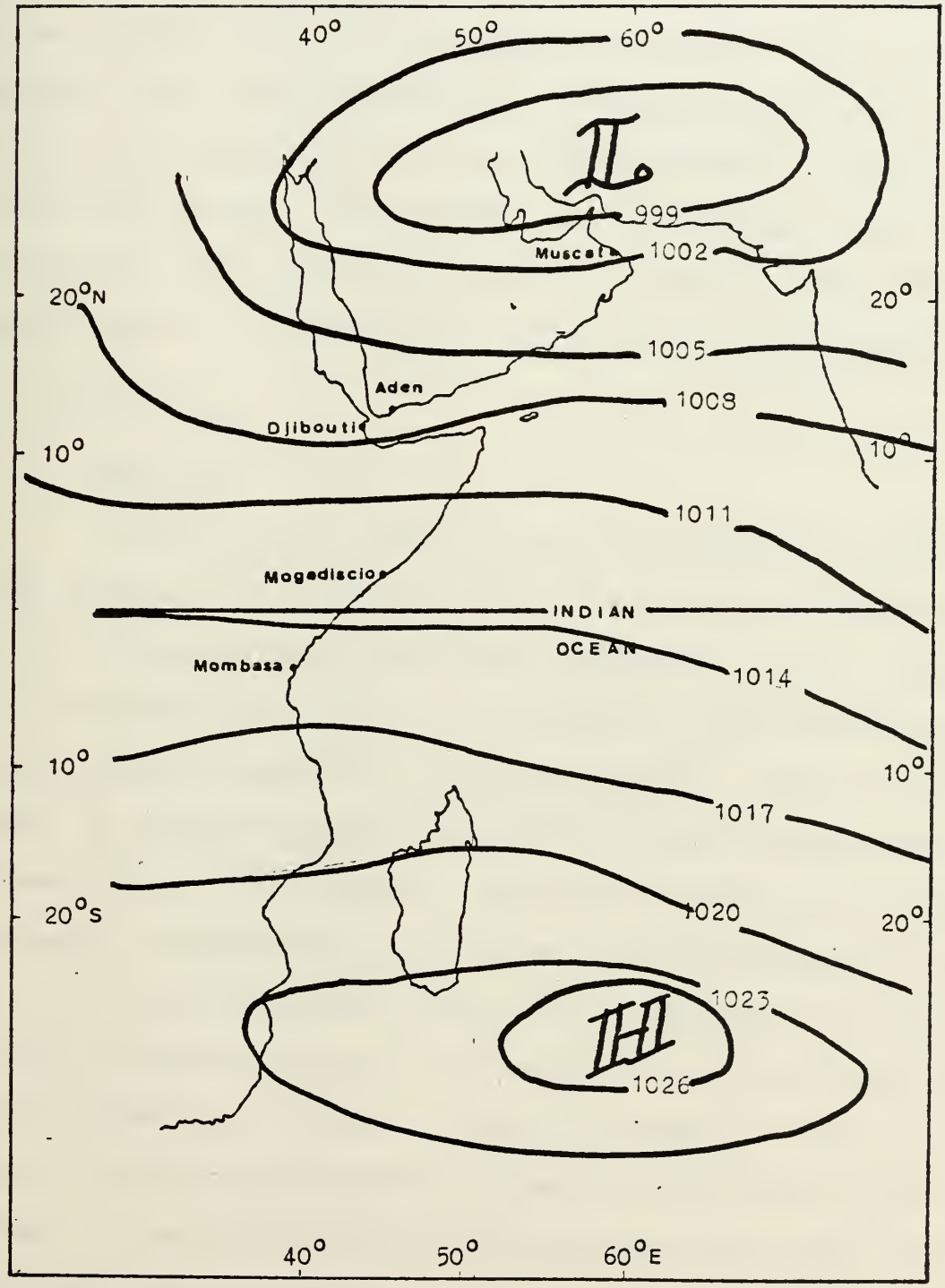

Figure 3. Pressure distribution during the summer monsoon [after Fairbridge, 1966].

weaken and the northeast monsoon dies. The southern hemisphere high pressure system intensifies and moves northward to the equator. A low pressure system develops over the hot Indian subcontinent. The southeasterly trade winds intensify, approach and cross the equator as southwesterlies and sweep across the Arabian Sea. The southwest monsoon is fully developed by mid-summer. This monsoon is very powerful with winds of 10.8-13.8 m/sec occurring 70% of the time and with seas greater than 2 m occurring 55% of the time (SP-68, HO-107).

D. CIRCULATION

1. General

Pickard [1975] describes the circulation of the Indian Ocean (Figure 4) as differing from that of the Atlantic and Pacific Oceans in its wind driven equatorial current system and its northern currents. The change of wind direction caused by the monsoon results in a current change. During the winter season a westward flowing North Equatorial Current exists between 8°N and the equator. From the equator to 8°S is the eastward flowing Equatorial Counter Current and south of this (to 20°S) is the westward flowing South Equatorial Current. During the summer monsoon the westward flow of the North Equatorial Current is reversed. This flow combines with the Equatorial Counter Current and is termed the Southwest Monsoon Current. A weak Equatorial undercurrent exists east of 60°E during the winter monsoon.

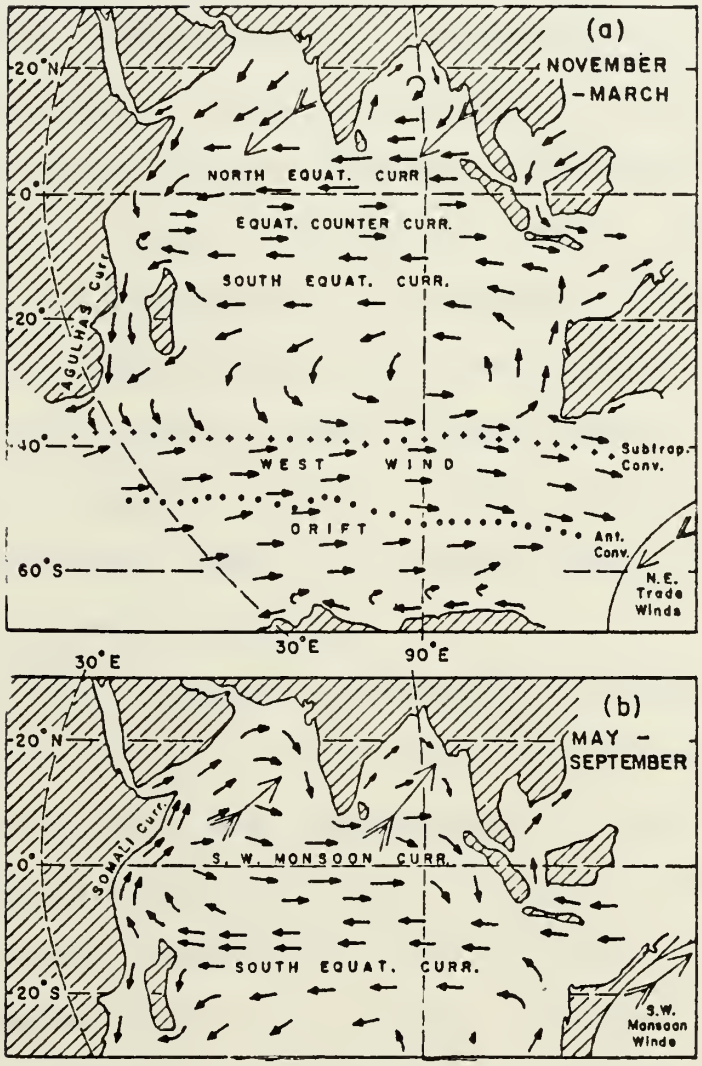

Figure 4. Surface circulation of the Indian Ocean (a) winter, (b) summer [from Pickard, 1975].

During the southwest monsoon, the South Equatorial Current provides a strong component to the north which forms the Somali Current.

2. Surface Circulation

During the winter monsoon, a southeasterly flow occurs along the Arabian coast. This is the Somali Current (also known as the Northeast Monsoon Current or Northeast Monsoon Drift). The Somali Current, during this season, follows the coast of Africa to approximately 2°S [Pickard, 1975]. HO-107 indicates current speeds of less than 50 cm/sec in the Somali Basin and 75 cm/sec along the east African coast. The Somali Current extends to depths of 200 m. North of 5°N a counter-current is found [Knox, 1980]. An eastward Equatorial Counter-current flows between 2° and 8°S.

Düing [1980] observed the reversal of the Somali Current during the spring of 1979 using direct measurement for periods of 14 to 24 days over three months (17 April - 30 July). This observation corroborated earlier studies [Leetmaa, 1972, 1973] which reported the transition of the Somali Current from a southerly flowing current to a strong northerly flowing current at 1°S by mid-April. The reversal was observed to pulsate rather than proceed as a continuous northerly flow of water. Knox [1980] suggests that this reversal begins in response to local wind changes rather than the onset of the summer monsoon.

Sverdrup et al. [1942] interpreted the Somali Current's response to the summer monsoon as a simple reversal of

current direction. Since the mid 1960's, and especially after the International Indian Ocean Expedition (IIOE) in the years 1962 to 1965, it has been recognized that the flow regime of the Somali Current during the summer monsoon is much more complicated. Offshore movement occurs as the current progresses, usually at headlands [Knox, 1980]. Wedges of cold upwelled water are apparent at these departures from the coast. These have been shown by Bruce [1979] to be part of a series of seasonally recurring eddies. The major departure of the current from the coast occurs near 10°N when the current is fully developed, but the point of separation does vary from year to year [Bruce, 1979].

The Somali Current in summer is quite intense with surface speeds of 200 to 350 cm/sec [Knox, 1980]. Following the separation from the coast, the flow forms the Southwest Monsoon current and crosses the northern Indian Ocean.

3. Subsurface Currents

Fairbridge [1966] describes the subsurface circulation of the Indian Ocean during the winter monsoon from geostrophic and direct measurements taken in 1960. At depths of 15 m, the current flow is similar to that of the surface, except that the Equatorial Counter-Current is considerably narrower than at the surface. Currents at 200 m are the reverse of those at the surface north of 5°N and east of 70°E. It has been noted that this eastern reversal is not always seen, however [Knox, 1980]. At 500 m the flow is generally easterly between 5°N and 10°S near the coast. A small anti-cyclonic gyre is found at 5°S, 60°E.

Measurements during one of the early studies of the summer monsoon [Swallow and Bruce, 1966] revealed strong subsurface flows, but these strong flows were extremely variable with no recognized circulation pattern. Later observations [Luyten and Swallow, 1976] revealed a persistent zonal flow which reversed at depth near the Equator. The circulation north of 3°N is unsettled but Leetmaa [1980] found a coherent coastal current flowing to the southwest between 3°N and 4°S.

The subsurface circulation during the winter is not well documented in modern literature. Fenner and Cronin [1978] discuss the presence of Red Sea Intermediate Water (RSIW), Persian Gulf Intermediate Water (PGIW), Subtropical Subsurface Water (SSW), and Antarctic Intermediate Water (AAIW) at a station located near 5°N off the east African coast. The presence of these water masses suggests a southerly flow between 250 and 400 m (advecting PGIW) and between 500 and 900 m (advecting RSIW) along the African coast. AAIW and SSW are advected northward along the coast by flows between 400 and 800 m.

E. EDDIES

Findlay [1866] wrote of a "giant whirl" off the east African coast. Since then, a major eddy has been recognized as a notable feature of the summer circulation. However, the existence of smaller eddies to the north and south of the main eddy was observed for four consecutive years [Bruce, 1979]. Figure 5 depicts the character of these eddy fields during the late summer of 1975, 1976 and 1977.

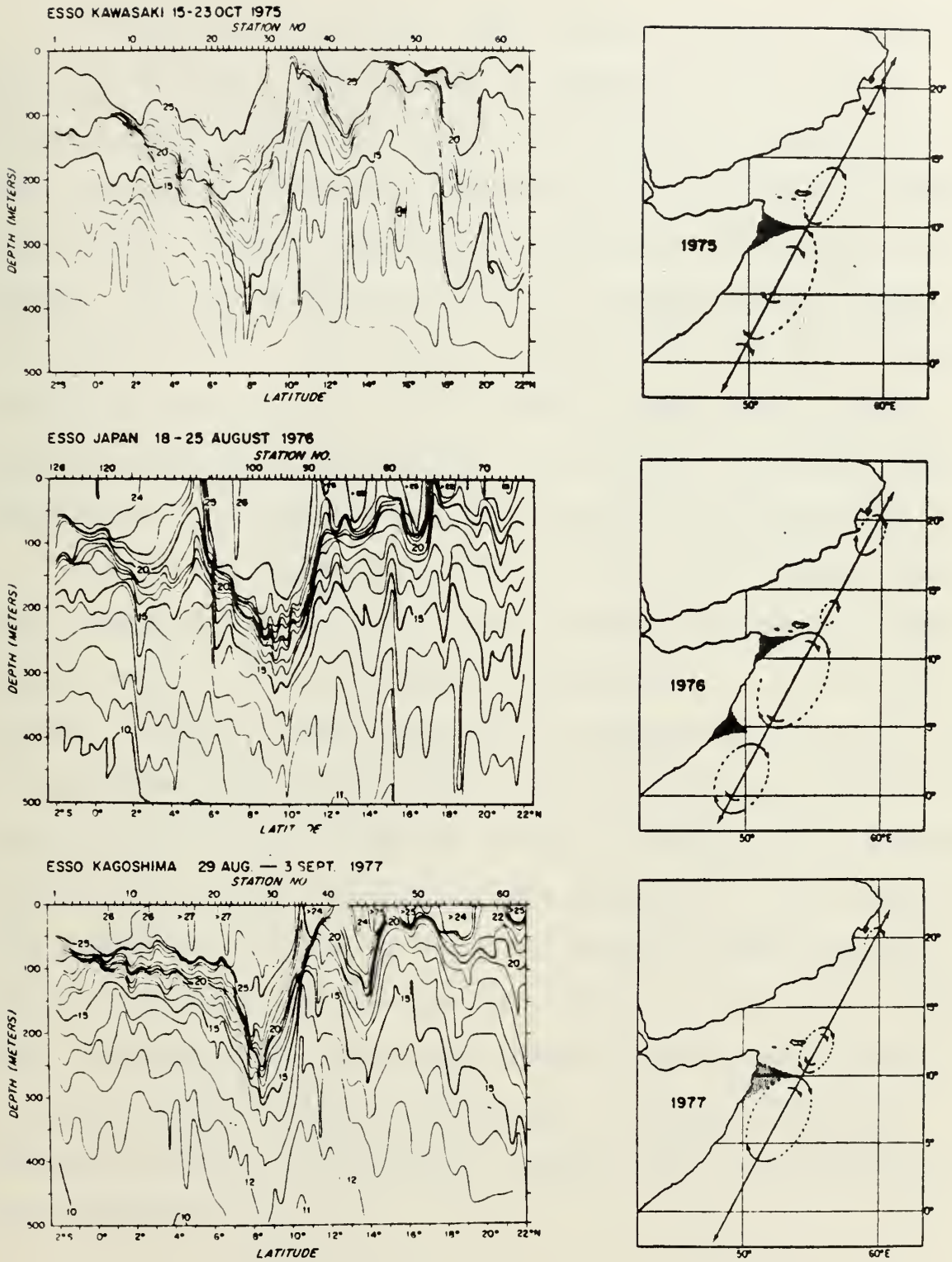

Figure 5. Cross section of eddy fields, 1975-1977 [from Bruce, 1979].

The largest warm core eddy, formed between 4°N and 12°N, is the first eddy to form in response to the summer monsoon. This major (or "prime" as Bruce [1979] calls it) eddy measures 400 to 600 km horizontally and extends to depths below 450 m. Deeper observations were restricted by XBT limitations. The major eddy can extend to depths greater than 1 km [Knox, 1980]. The smaller southern eddy was not observed to develop every year as did the smaller eddy to the north. Bruce's data indicated that once the general circulation was established, it continued for the duration of the monsoon.

With the weakening of the monsoon in the autumn, the eddy system begins to relax. Bruce observed evidence of the "prime" eddy into late January, the beginning of the winter monsoon. Figure 6 shows the eddy development during 1978. As the southwest monsoon dies, the thermocline begins to shoal in the body of the eddy (November panel). However, the depressed thermocline is still visible in late December. Data taken by USNS KINGSPORT in March 1977 for the BEARING STAKE exercise [Fenner and Cronin, 1978] does not reveal an eddy field. However, the temperature structure observed during this period was warmer than the ICAPS climatology. This may indicate lingering effects of the strong "prime" eddy in the summer of 1976 (Figure 5).

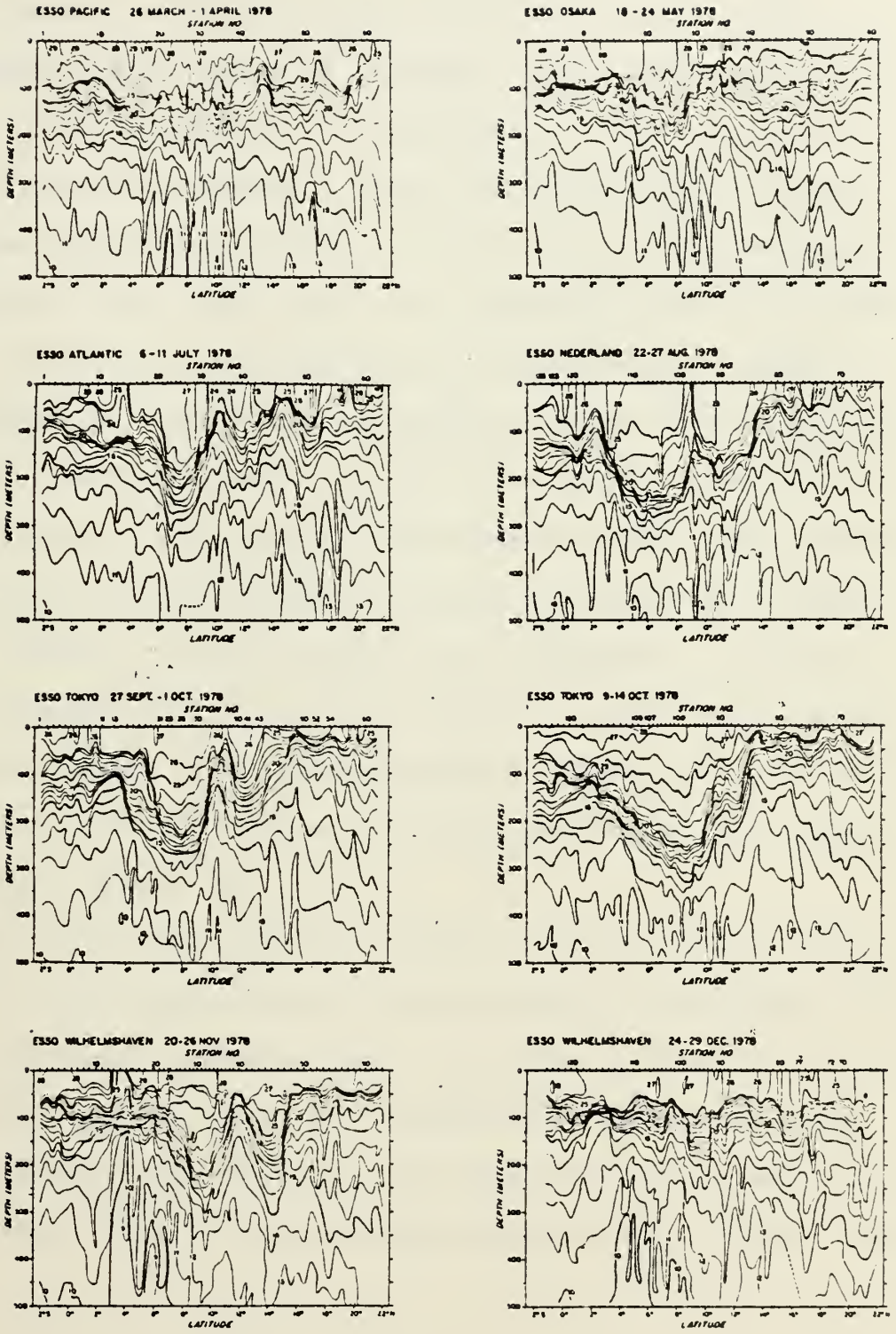

Figure 6. Development of the eddy field, 1978 [from Bruce, 1979].

F. MIXED LAYER DEPTH

The annual variation of the mixed layer depth (MLD) in the western Indian Ocean is reversed from that normally experienced in mid-latitudes; the MLD shoals in the winter and deepens during the summer. Strong turbulent mixing during the summer monsoon undoubtedly contributes to the deepened MLD. The surface layer cools during the summer by 2° to 3°C [Knox, 1980]. The mechanism by which this cooling takes place is still unknown. Knox [1980] hypothesizes that during summer the Somali Current advects cooler water from the south and that eddies may be forced by, or separated from, the main current and move to the interior, decaying as they go. Bruce [1979], however, did not observe this migration. Figure 7 depicts the MLD during July and August. In the Somali Basin depths can exceed 120 m during August. This occurs at the approximate position of the main eddy feature of the summer circulation (Figure 5).

During the winter the MLD shoals to 60 m south of 10°N and to 40 m along the African coast south of the equator (Fig. 8). It has been suggested that a possible mechanism for this shoaling of the MLD could be the advection of warmer water from the Arabian Sea region or the remnants of the warm core eddies formed during the preceding summer months [Knox, 1980].

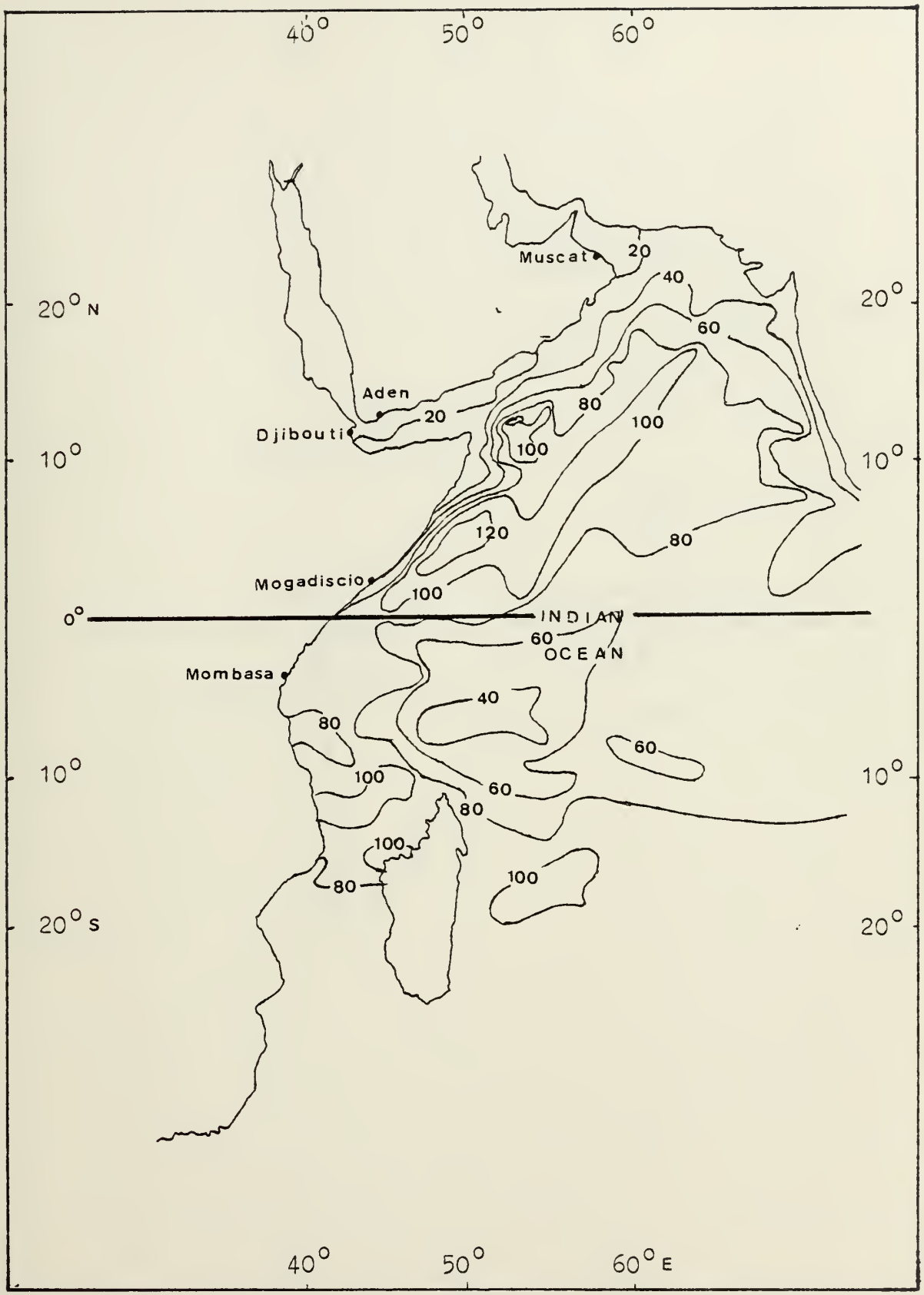

Figure 7. Mixed Layer Depth (meters) in July and August [after Wyrtki, 1971].

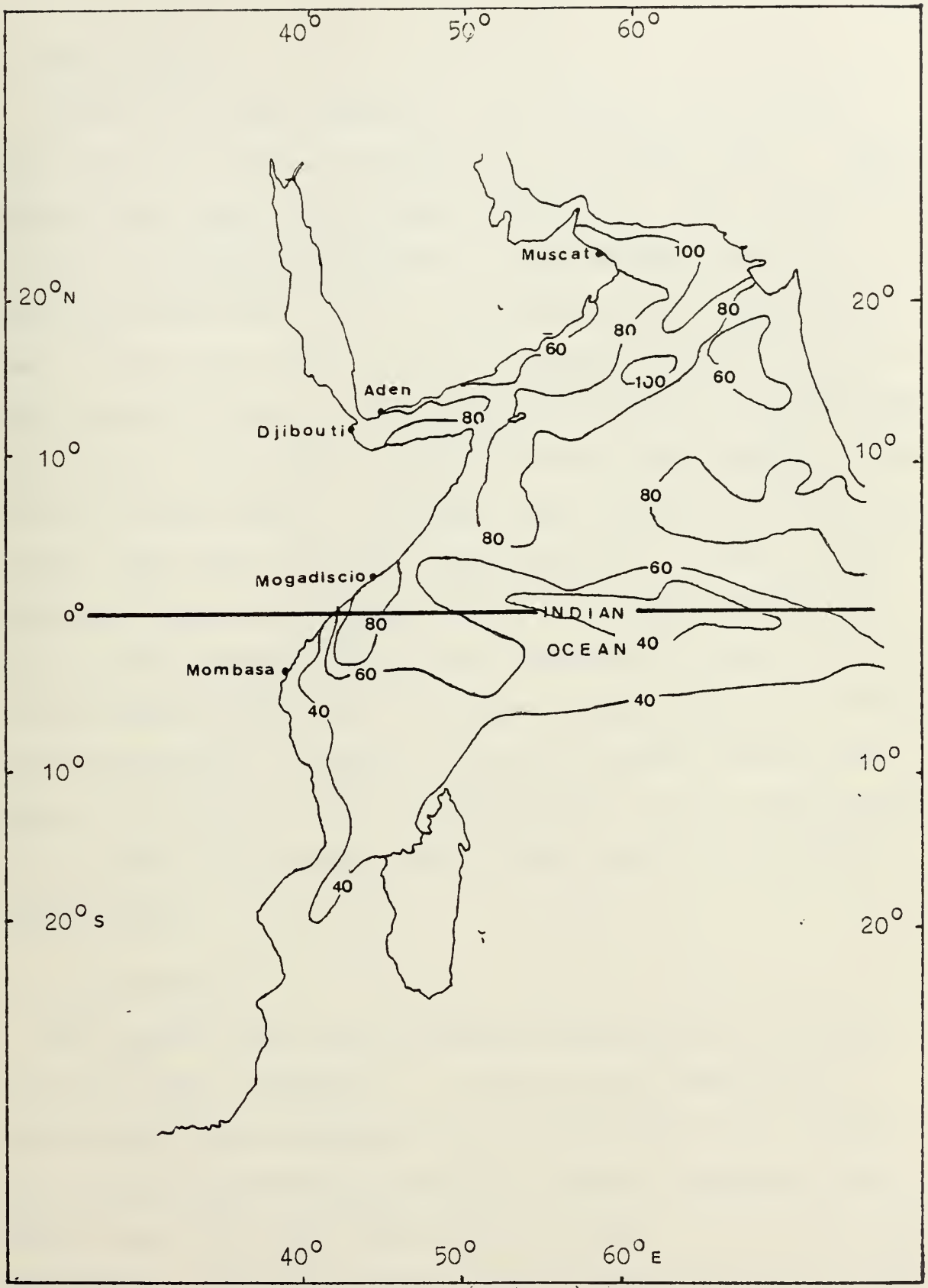

Figure 8. Mixed Layer Depth (meters) in January and February [after Wyrtki, 1971].

G. DEPTH EXCESS

Contours of depth excess for each season in the western Indian Ocean are shown in Figures 9-12 [Colborn, 1976]. Depth excess is the depth greater than the critical depth (depth at at which sound speed equals that at the surface) and is a necessary requirement for CZ (convergence zone) propagation. When an SSP (sound speed profile) is bottom limited (i.e., no depth excess exists), a bottom conjugate depth can be computed which defines the limits of the DSC (deep sound channel). The bottom conjugate depth is the depth near the surface which has a sound speed equal to that at the sea floor. Colborn [1976] shows that depth excess exists only in the Somali Basin and that bottom limited conditions are expected to occur only during the spring (Figure 10). However, Fenner and Cronin [1978] found depth excess to exist, to varying degrees, during this season in the Somali Basin. The bathymetry of the ridge system to the north of the Somali Basin causes the SSP to be bottom limited there.

H. WATER MASSES

The general water mass structure as presented by Pickard [1975] is shown in Figure 13. Surface water masses have a substantially zonal distribution of properties with a temperature maximum near the equator and a salinity maximum in the Arabian Sea (36.5 ‰). The salinity maximum is due to extreme evaporation. Below the surface layer, Indian Equatorial Water

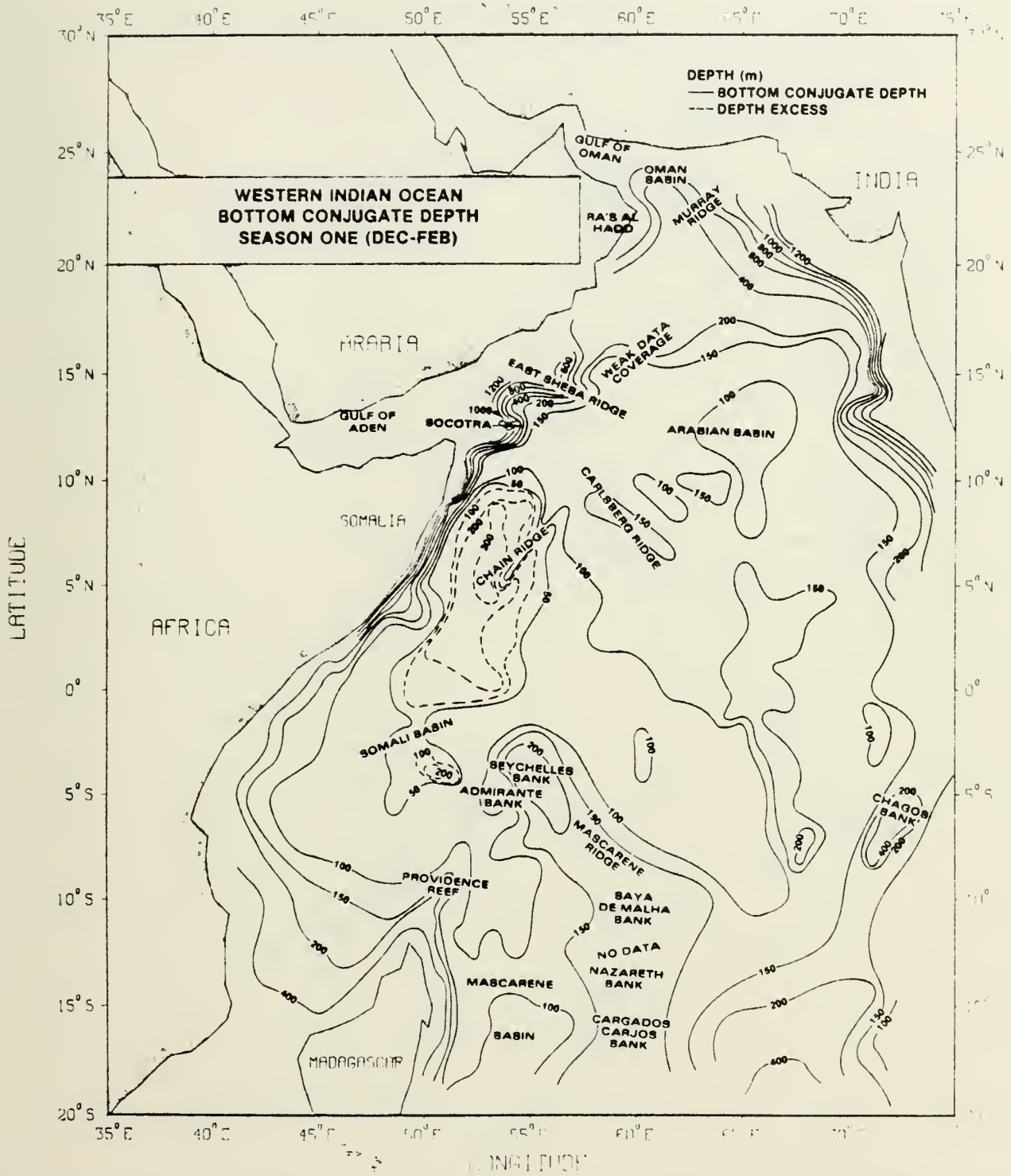

Figure 9. Bottom conjugate depth (winter) [from Colborn, 1976].

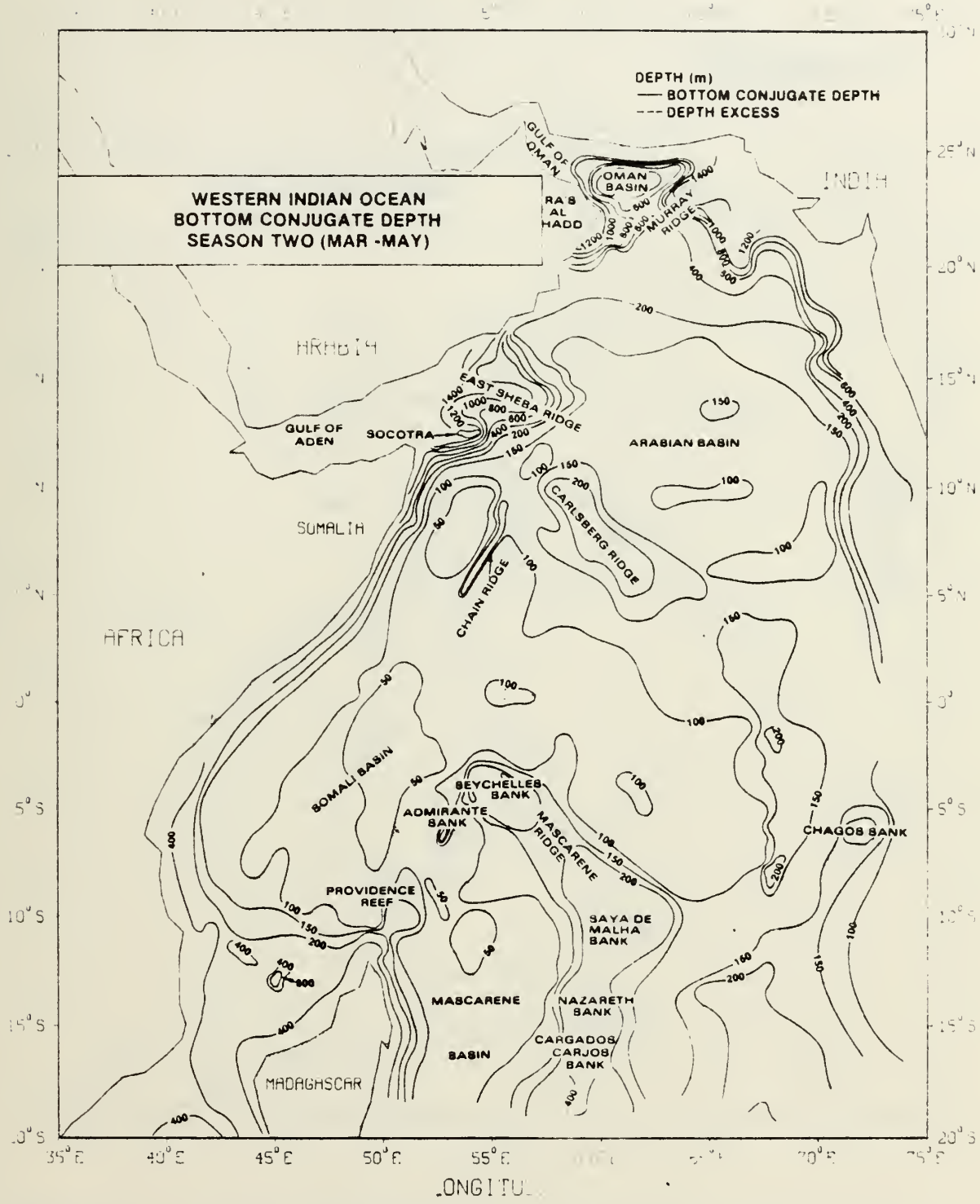

Figure 10. Bottom conjugate depth (spring) [from Colborn, 1976].

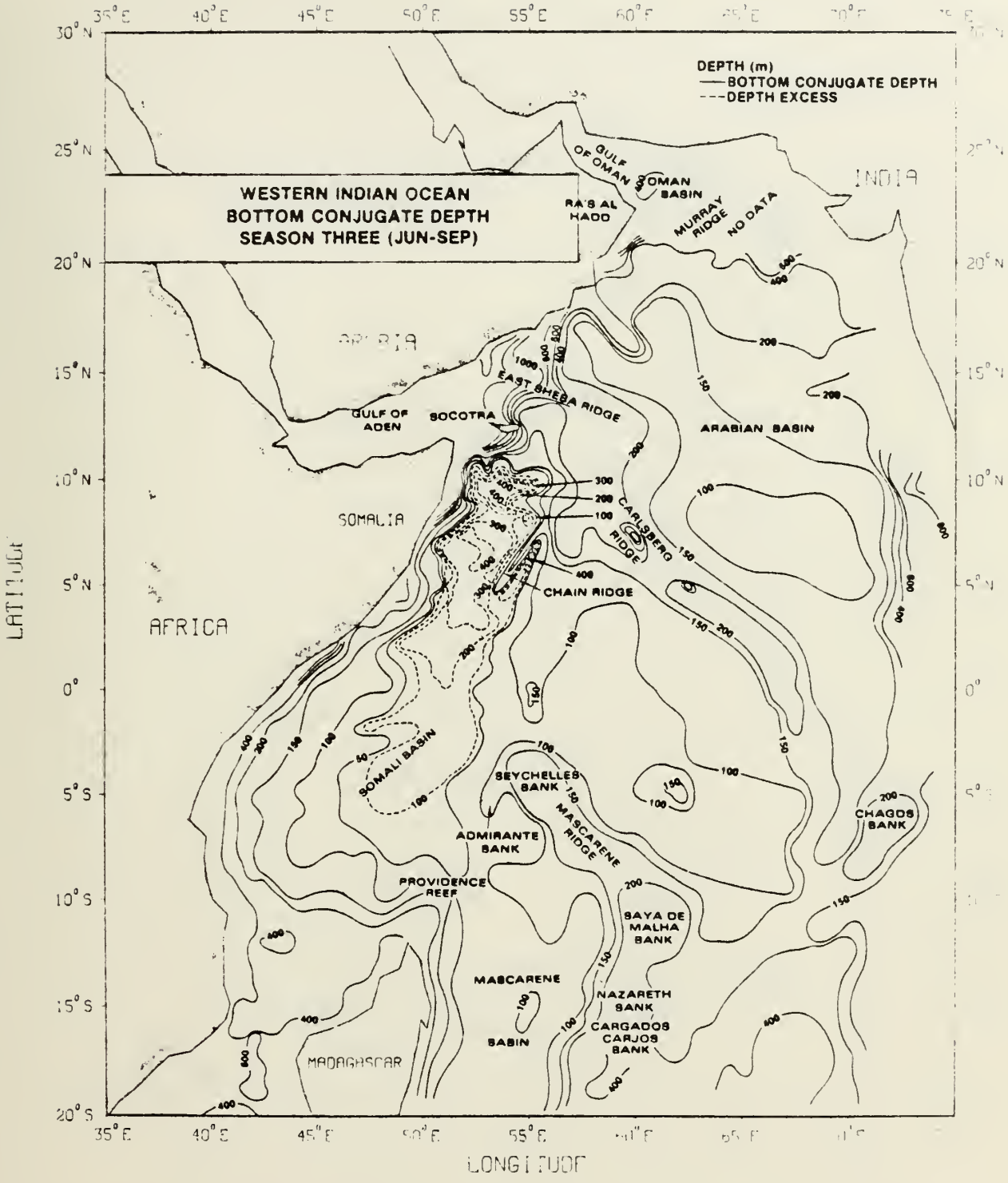

Figure 11. Bottom conjugate depth (summer) [from Colborn, 1976].

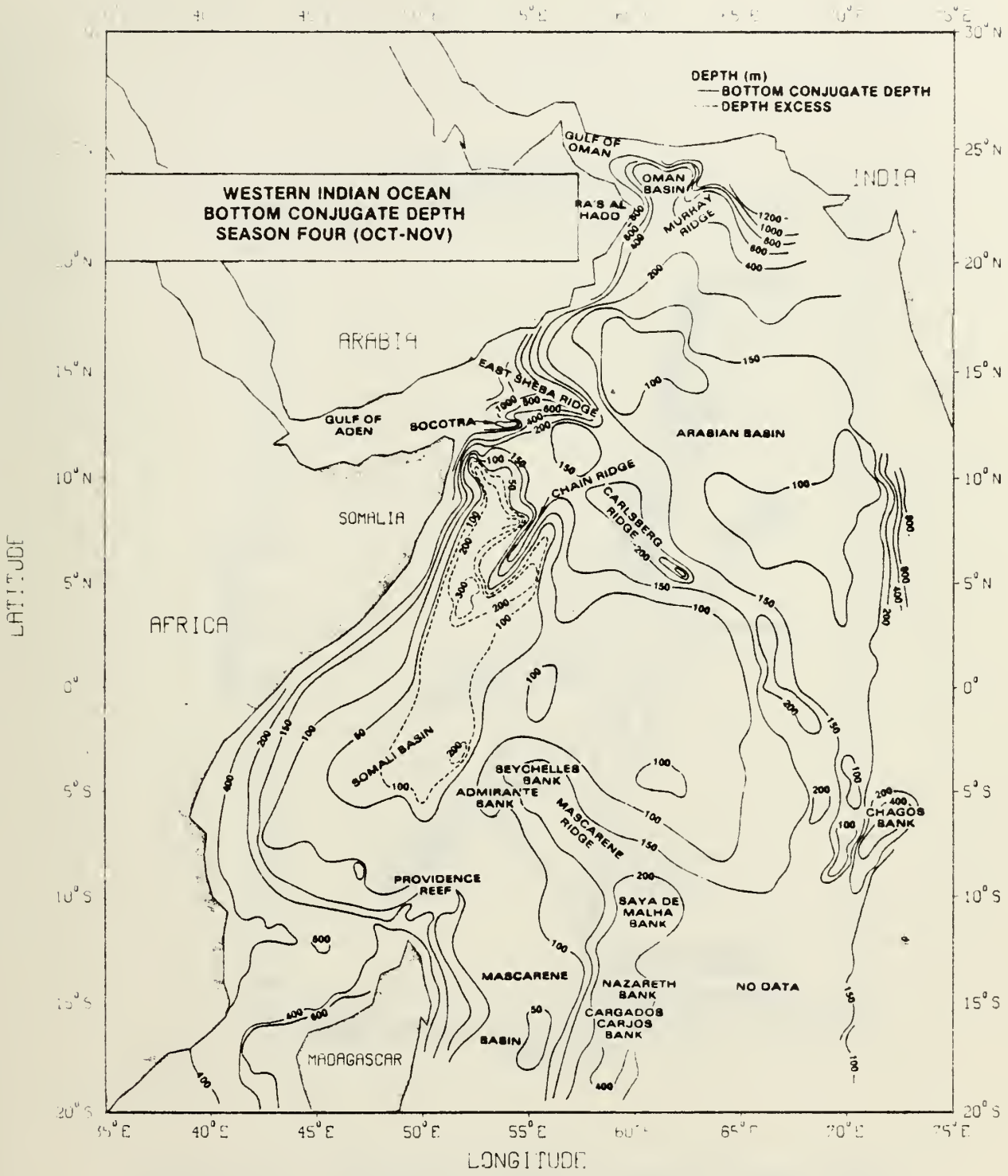

Figure 12. Bottom conjugate depth (fall) [from Colborn, 1976].

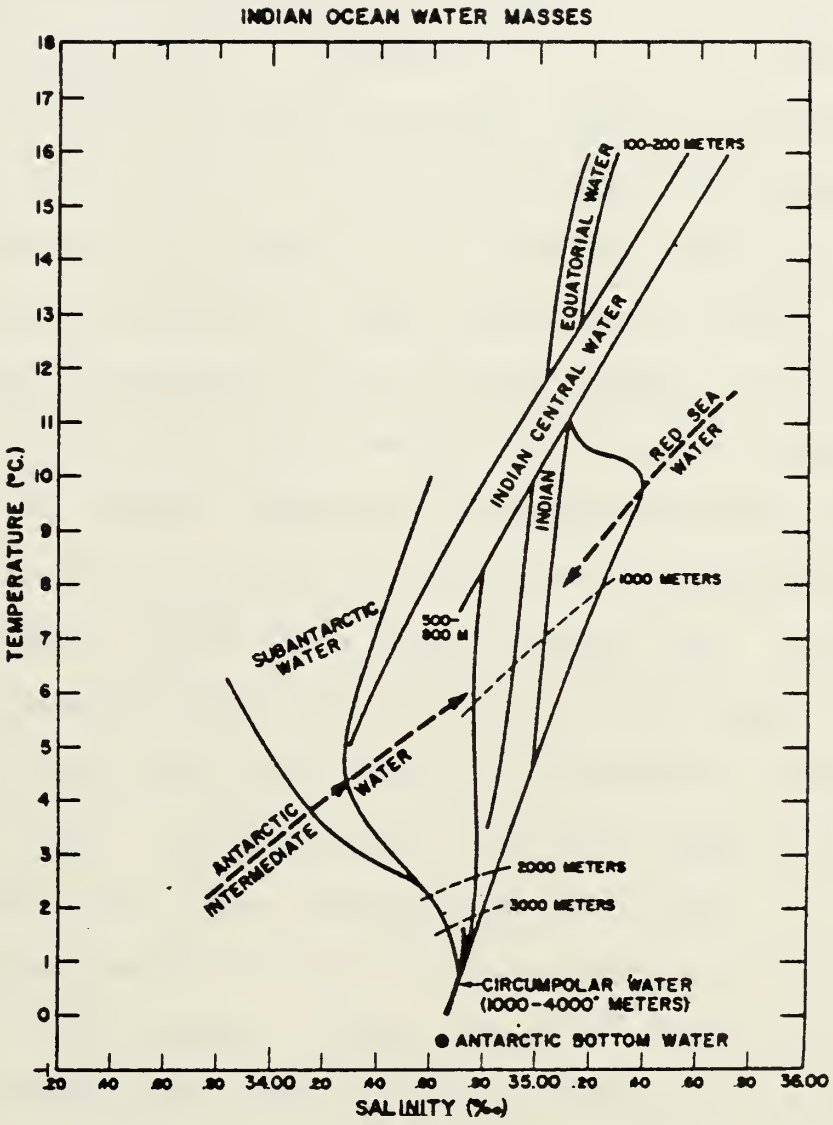

Figure 13. Classical view of Indian Ocean water mass structure [after Sverdrup et al., 1942].

with salinities ranging from 34.9 to 35.5‰ is found. Some of this water is formed in the Arabian Sea, the Red Sea and Persian Gulf. Both Deep and Bottom Waters are products of waters found in the Southern and Atlantic Oceans. Indian Ocean Deep Water is characterized by a temperature of 2°C and a salinity of 34.8‰ . Red Sea Intermediate Water (RSIW) is an identifiable feature of the Arabian Sea and northern Indian Ocean. It penetrates southward to about 25°S at 1000 m. RSIW has a characteristic temperature of 15°C and a salinity of 36‰ .

An extensive examination of the water masses of the western Indian Ocean during the summer monsoon of 1964 was conducted by Warren et al. [1966]. Figures 14 through 20 show temperature and salinity cross sections for several transects taken across the western Indian Ocean during August 1964. The surface waters presented some difficulties in that temperatures and salinities were not sufficiently conservative to adequately define water types. Two distinctly different types of surface waters were observed; warm, saline water ($T > 24°C$, $S > 35.7‰$) from the Arabian Sea and the Gulf of Aden (Stations 62 and 63, Figures 20a,b), and cooler, fresher water ($T < 22°C$, $S < 35.3‰$) carried northward by the Somali Current (Stations 64 and 65, Figures 20a,b).

Salinity structures for intermediate waters were found to be very disorderly. Generally, a low salinity layer overlay a high salinity layer. The lowest salinities ($< 35.2‰$) were found between 200 and 650 m with an average depth of 450 m

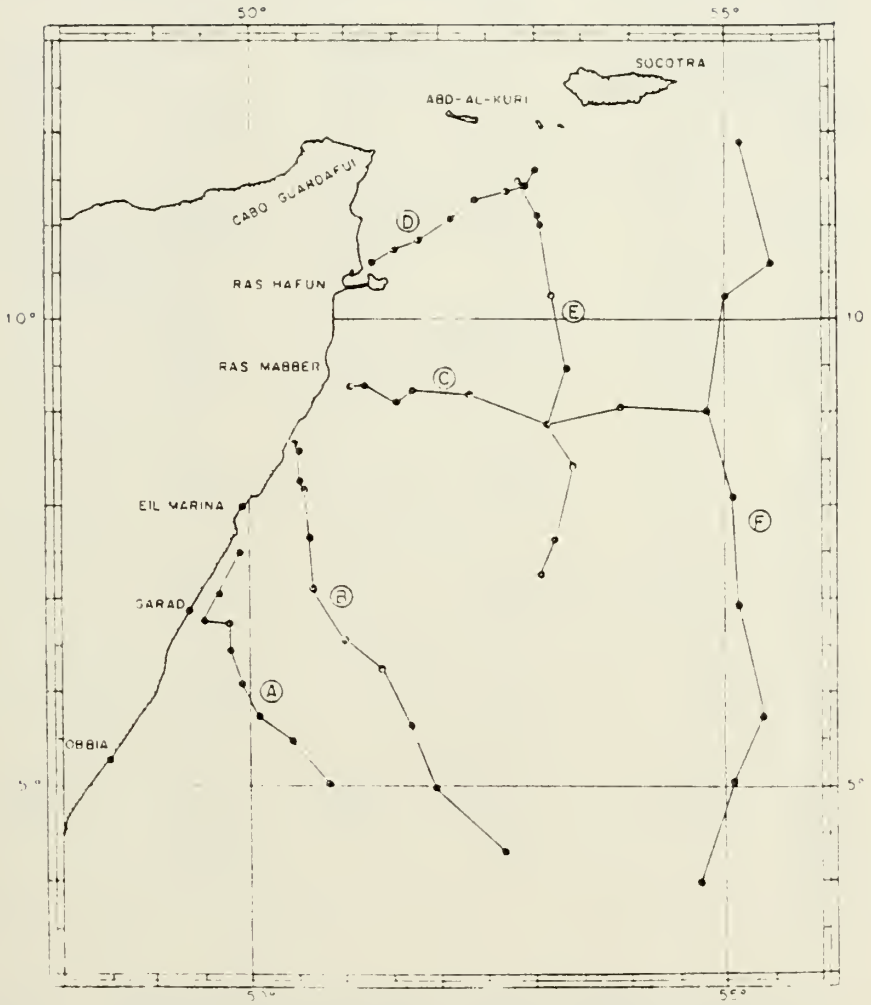

Figure 14. Location and designation of temperature-salinity profiles obtained during August 1964. Dots indicate station locations [after Warren et al., 1966].

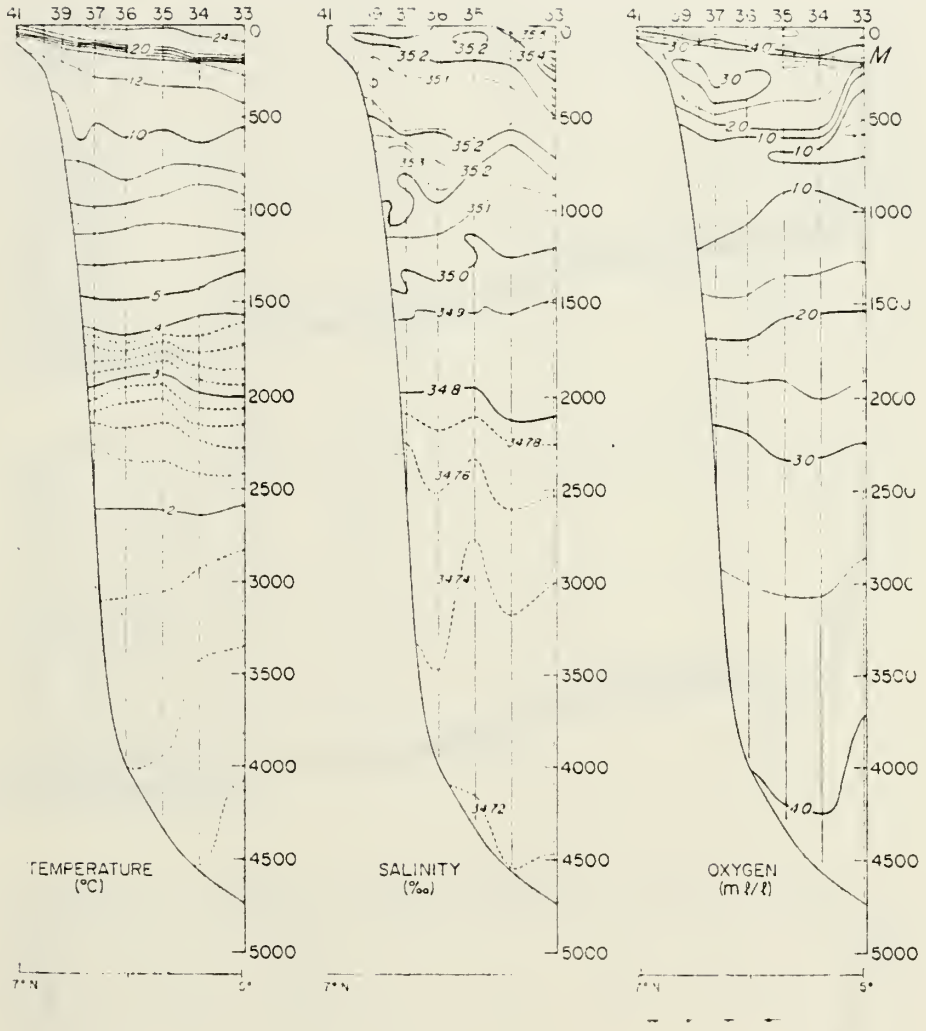

Figure 15. Property profiles for cross section A [after Warren et al., 1966].

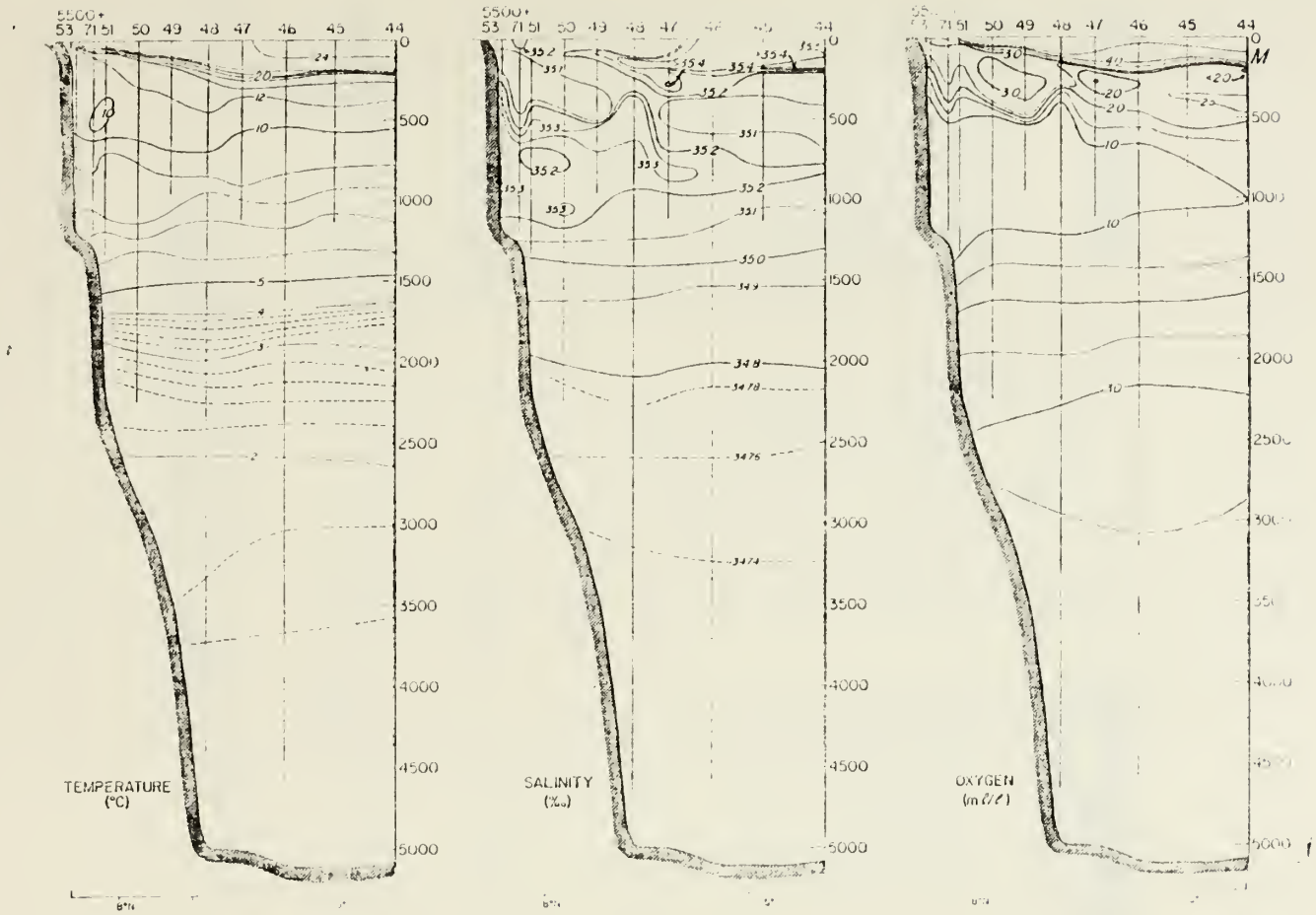

Figure 16. Property profiles for cross section B [after Warren et al., 1966].

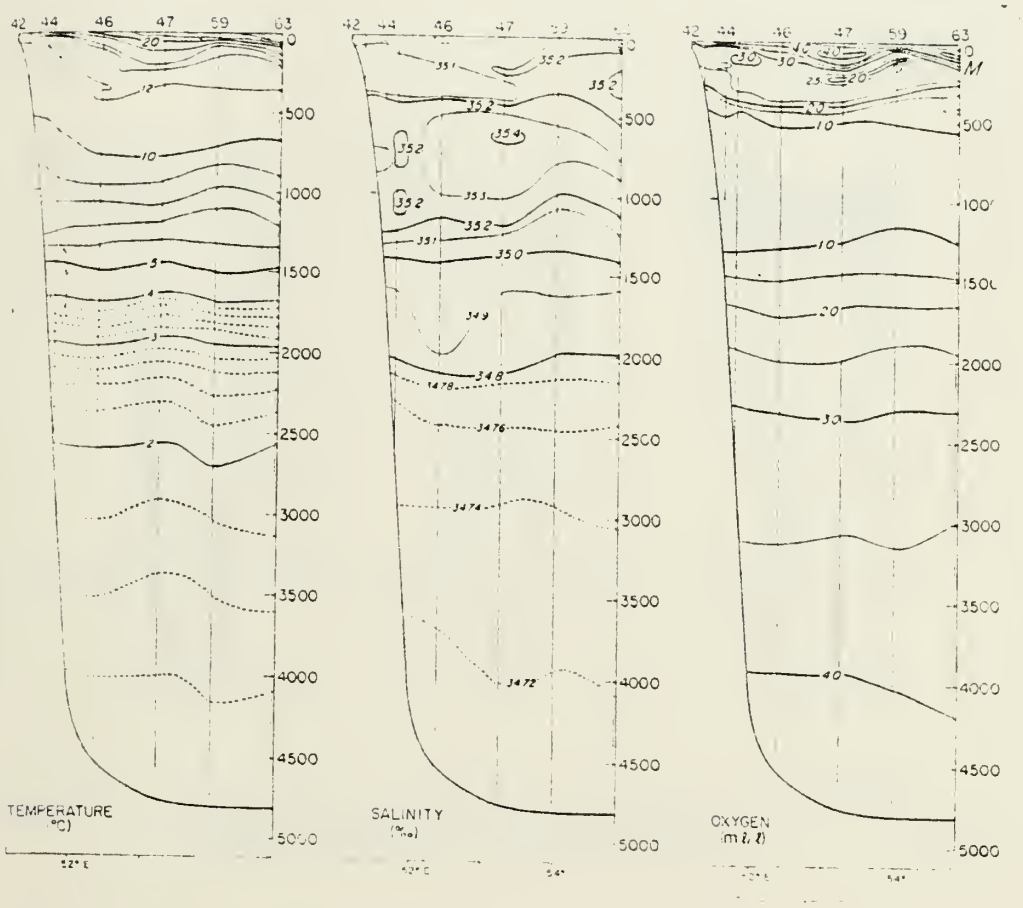

Figure 17. Property profiles for cross section C [after Warren et al., 1966].

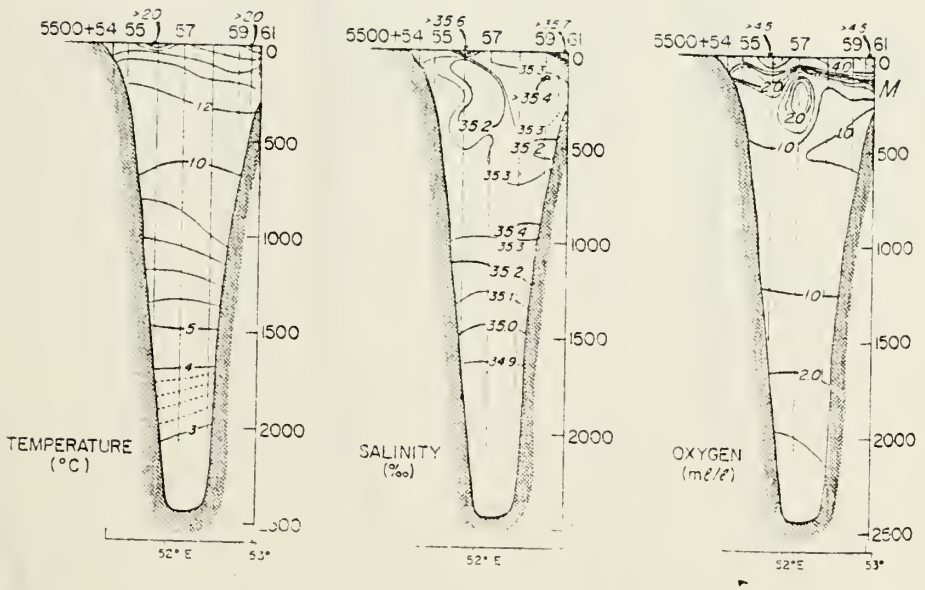

Figure 18. Property profiles for cross section D [after Warren et al., 1966].

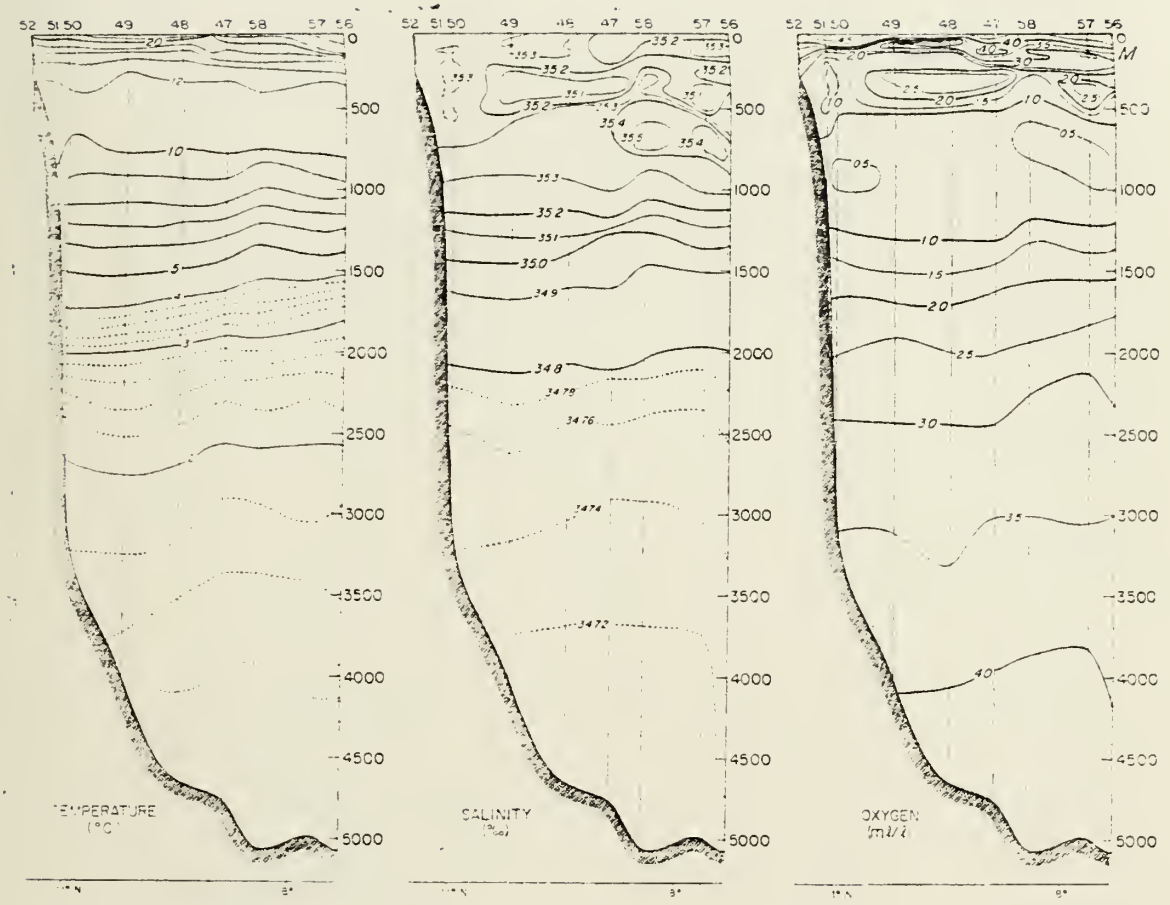

Figure 19. Property profiles for cross section E [after Warren et al., 1966].

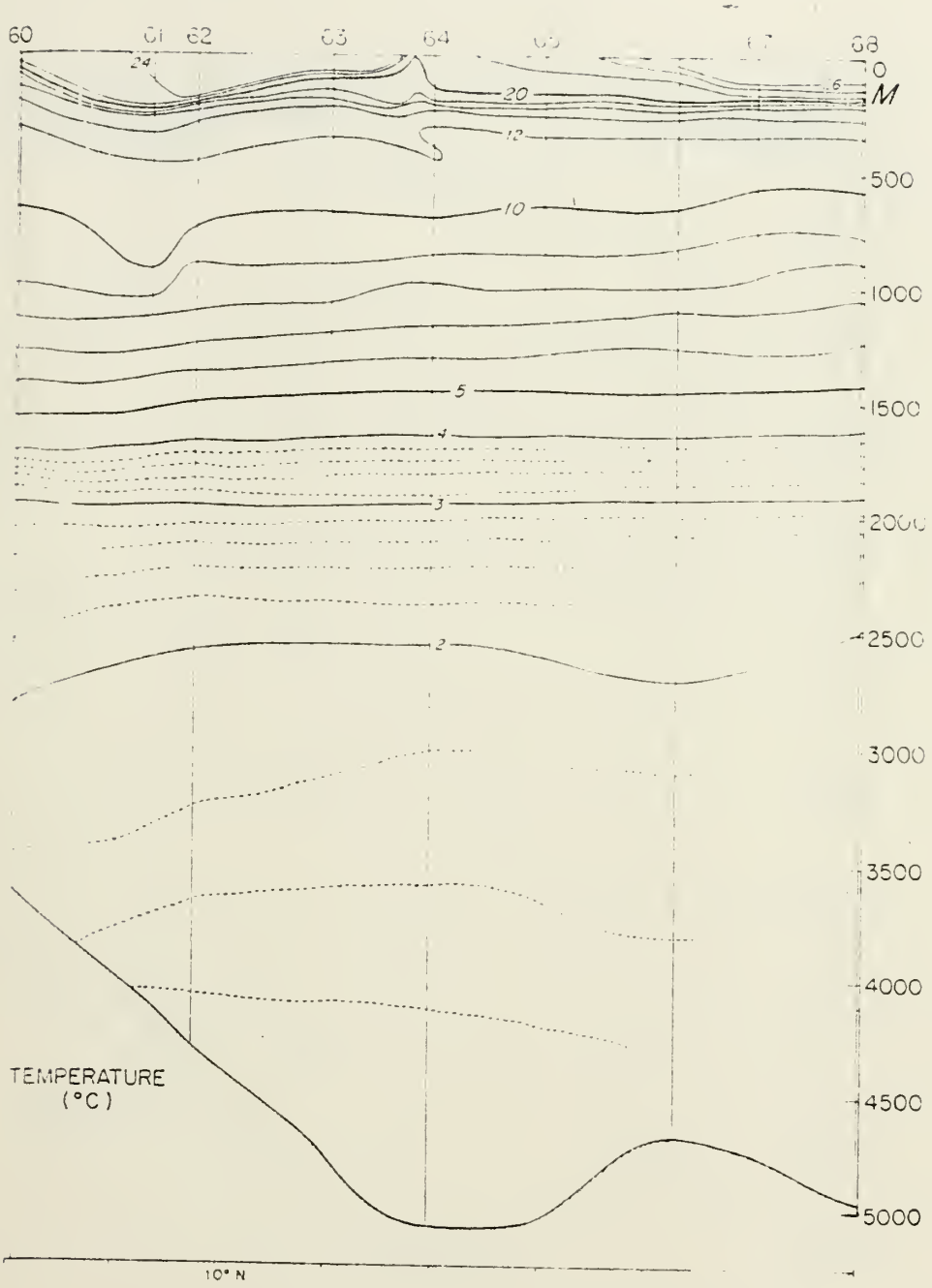

Figure 20a. Temperature profile for cross section F [after Warren et al., 1966].

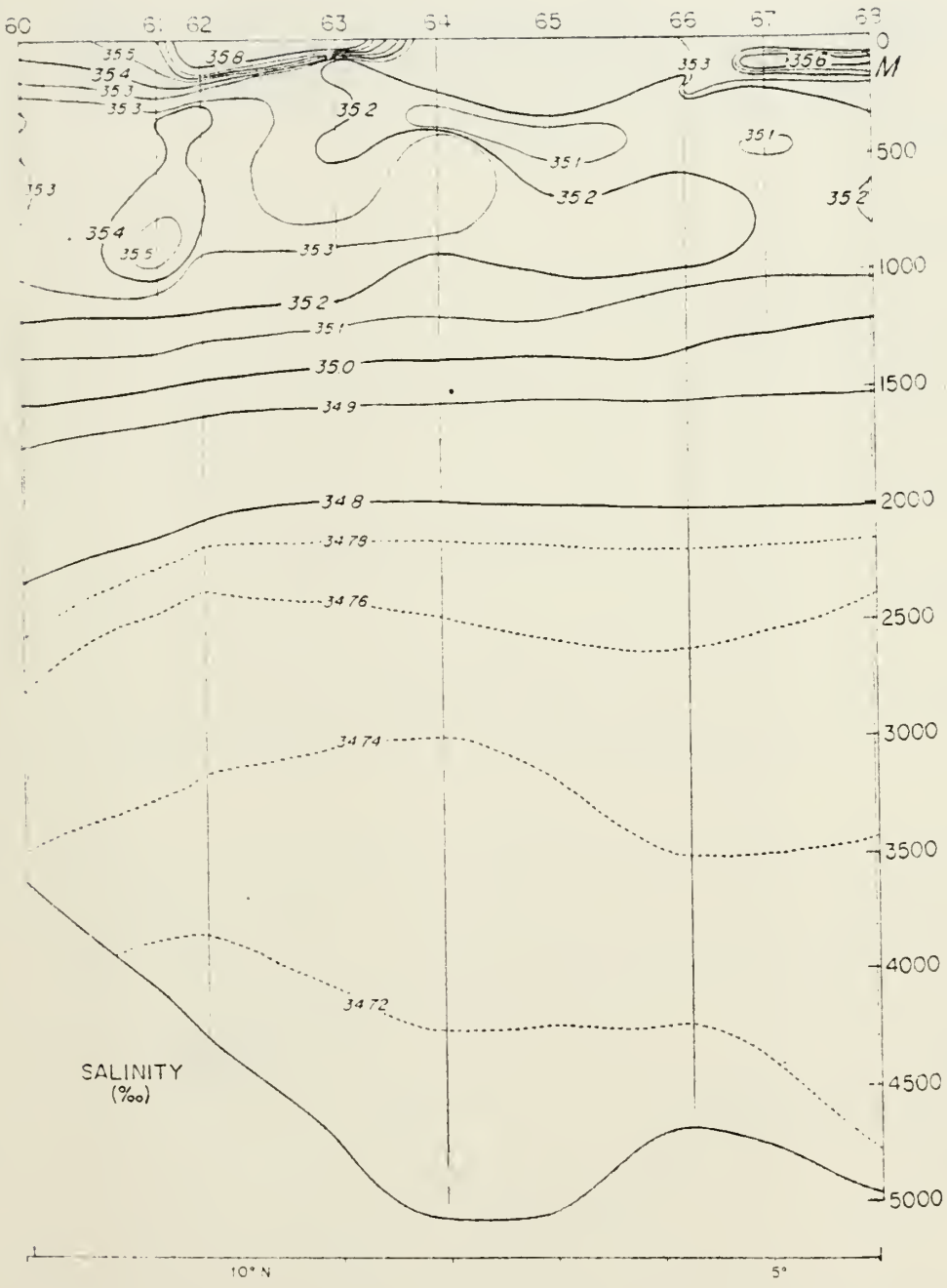

Figure 20b. Salinity profile for cross section F [after Warren et al., 1966].

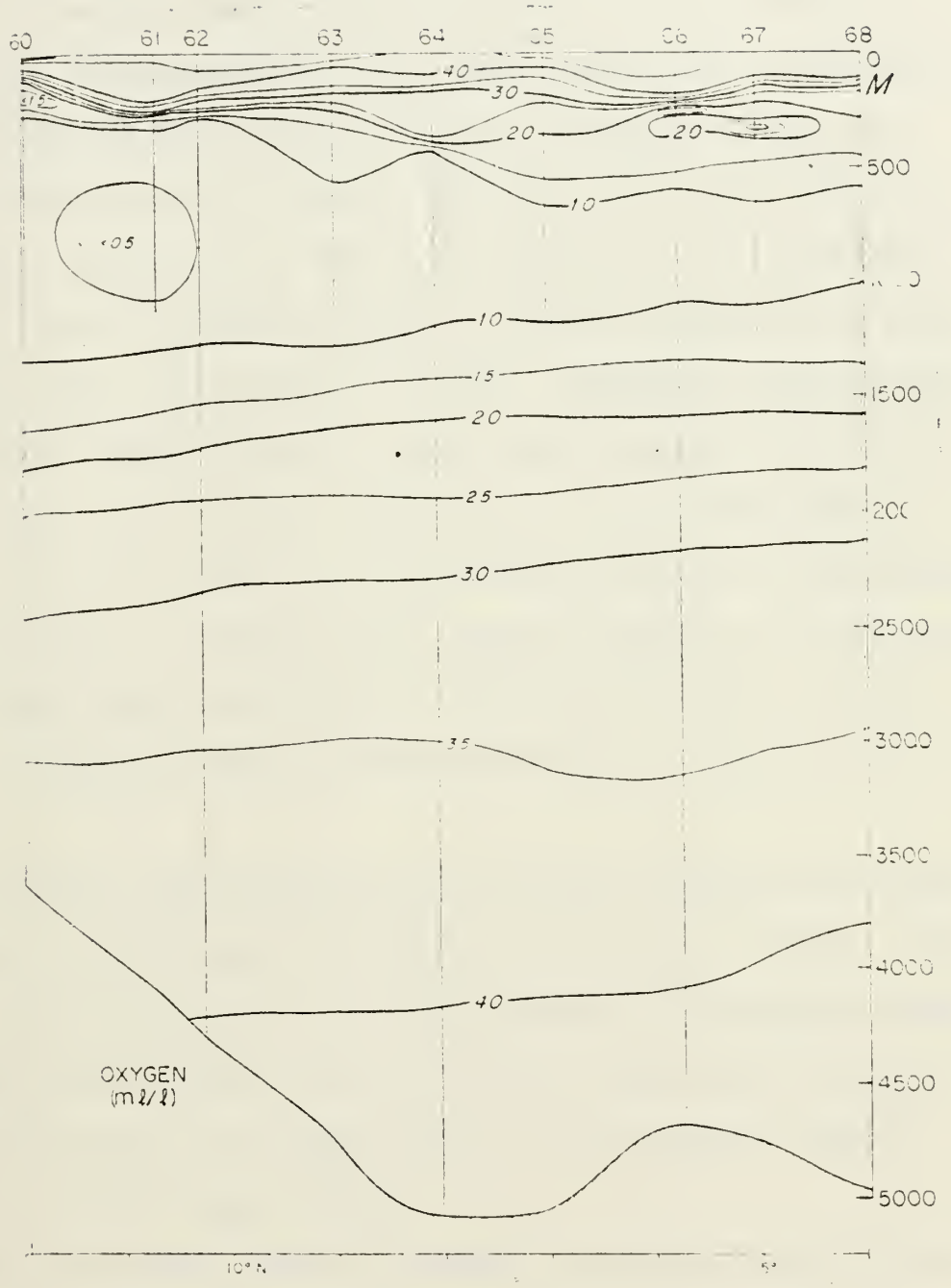

Figure 20c. Dissolved-oxygen concentration profile for cross section F. [after Warren et al., 1966].

(Figures 17 and 19). Highest salinities were found between 550 and 950 m with an average depth of 760 m (Figures 17 and 18). The dissolved oxygen concentration was the reverse of the salinity distribution; i.e., high salinities are associated with low oxygen levels and vice versa (Figures 17 and 18).

The irregularities found in Warren's study were due to a complicated intermingling of water masses at various depths. Because of these irregularities, it was not possible to draw inferences about the pattern of flow. Elaborate interleaving of relatively fresh, high O_2- level water masses and saline, low O_2- level water masses take place in the Somali Basin. Between σ_t of 26.4 and 27.0, Persian Gulf Water and Subtropical Subsurface Water, together with a small component of Equatorial Pacific Water from the Banda Sea, were interleaved. Interleaving of RSIW and AAIW occurred between σ_t values of 27.0 and 27.6.

Below these intermediate waters, North Indian Ocean Deep Water with $\sigma_t < 27.6$ and salinity of 35.1‰ was found. The source of this deep water was the Antarctic Circumpolar Water. Entrainment from the Red Sea and Persian Gulf water outflow caused salinities of the Deep Water to be slightly higher ($\sim$.02‰) in the Somali Basin.

Fenner and Cronin [1978] examined the water mass structure of the intermediate depths in conjunction with the BEARING STAKE exercise conducted in March 1977. They observed five water masses in the Somali Basin (see Figure 21):

1) High salinity Persian Gulf Intermediate Water with a core at 250 to 400 m.

2) Low salinity Subtropical Subsurface Water at depths of 400 to 500 m.

3) High salinity Red Sea Intermediate Water with a core between 500 and 900 m.

4) Low salinity Antarctic Intermediate Water between 700 and 800 m.

5) Low salinity Banda Intermediate Water found between 900 and 1000 m.

Values for deep waters shown in Figure 21 are the same as those for the summer season.

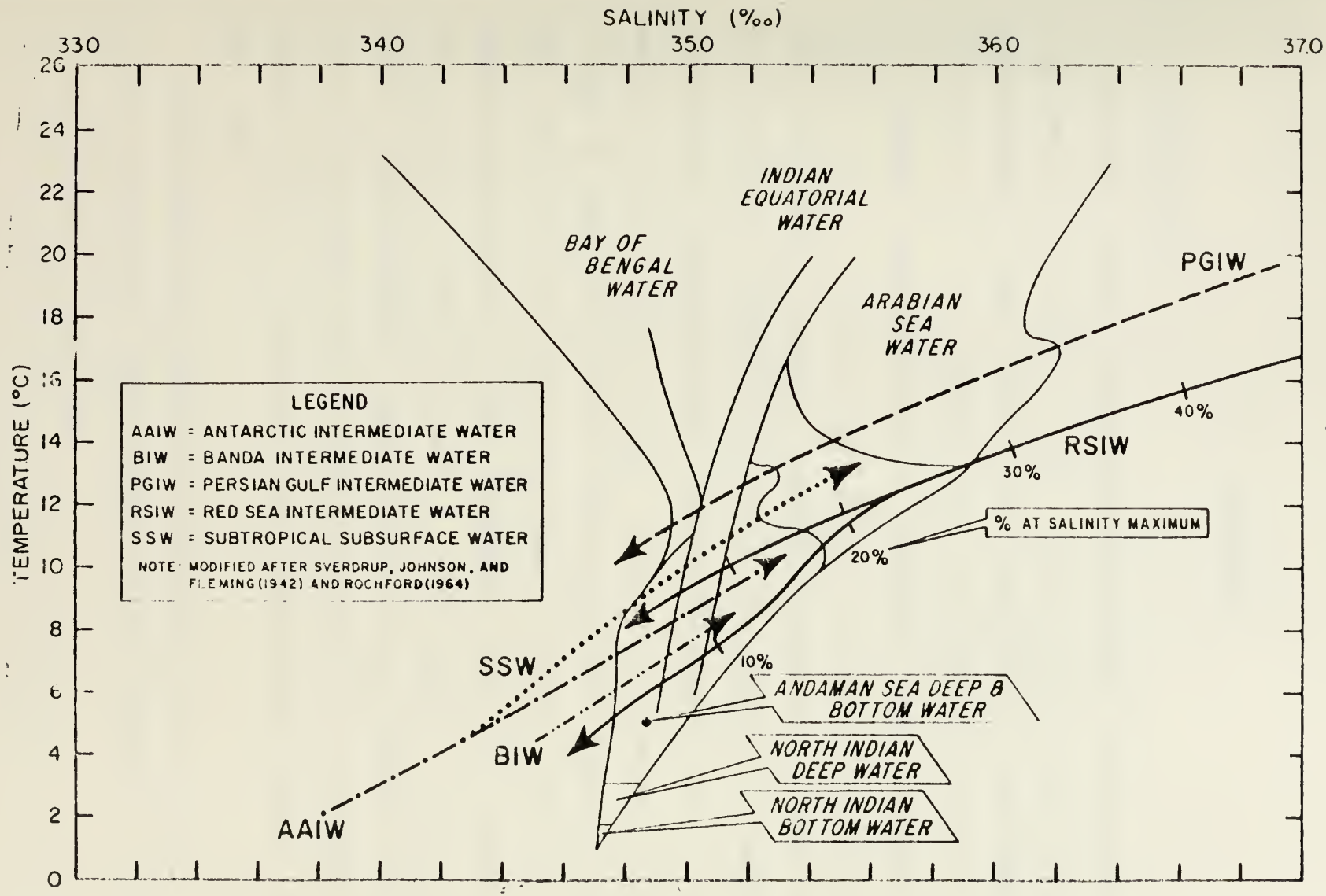

Figure 21. Water mass relationships in the north Indian Ocean [from Fenner and Cronin, 1978].

III. ACOUSTICS

A. INTRODUCTION

Data for acoustic analysis were obtained from two sources: 1) thermal traces taken by USNS KINGSPORT during March 1977 and supplied by NORDA (Naval Ocean Research and Development Activity); and, 2) a thermal field generated from XBT's dropped by a research team placed aboard the ESSO JAPAN in August 1976 [Bruce, 1979]. For the summer season, eleven thermal profiles were constructed to examine acoustic propagation within three environmentally different areas: 1) the middle of an eddy; 2) shoaling thermocline near the edge of an eddy; and, 3) cold upwelling areas outside an eddy. Figure 22 shows the location of each of these profiles and their position relative to the eddy fields observed during the summer of 1976. Figure 23 depicts the track of the USNS KINGSPORT during the winter and the position of XBT drops used in this analysis. Because of a lack of environmental features (such as the summer eddy field during the winter) and the sparcity of data, all available KINGSPORT XBT's in the same general area as the summer track were used.

Depth excess was observed at Stations A, B, C, D, E, F, G, H and I during the summer season and at Stations 2, 3, 4, 5, 6, 7,and 8 during the winter.

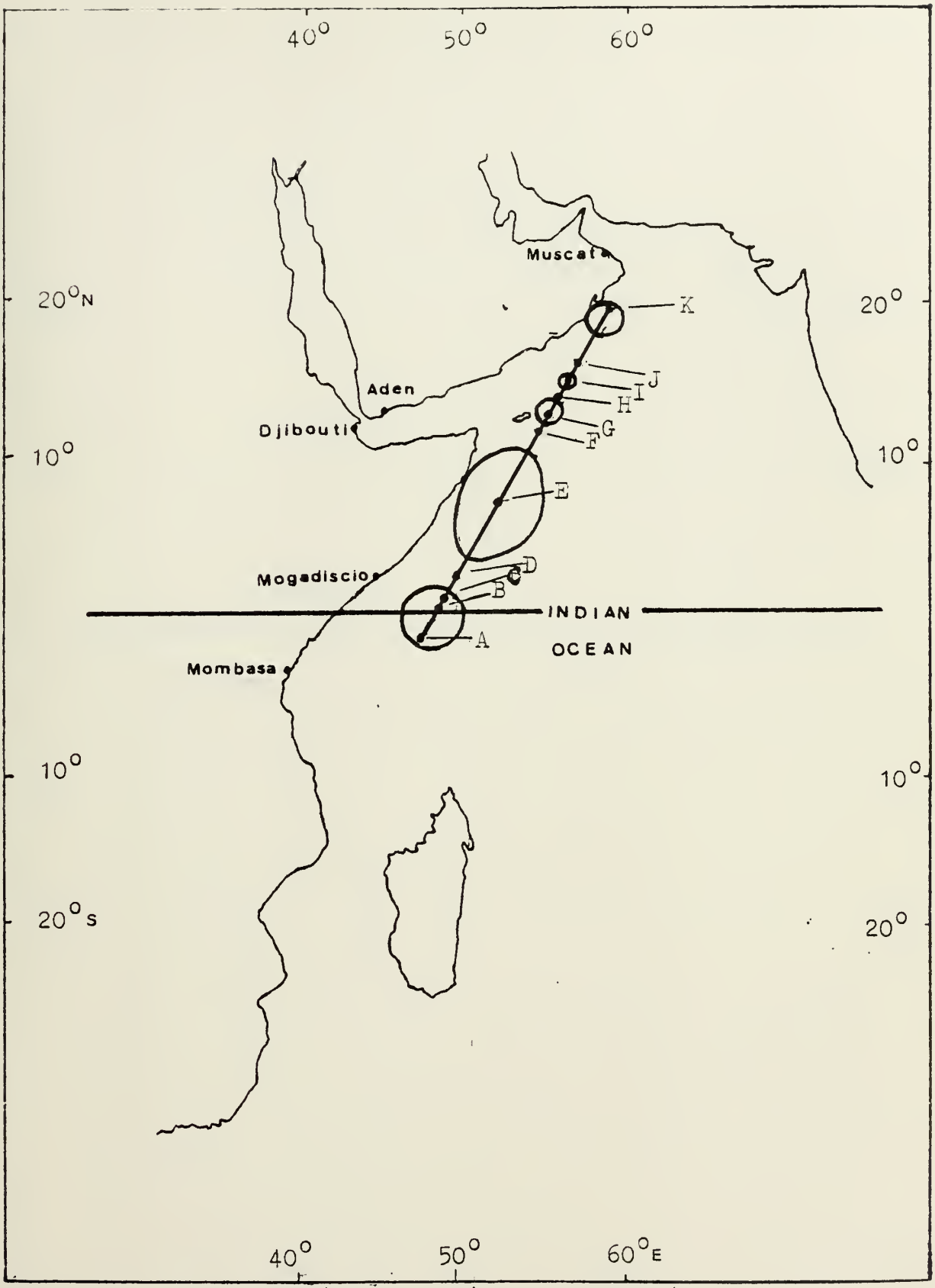

Figure 22. ESSO JAPAN track and profile locations. The circles indicate the general location of warm core eddies in August 1976 [after Bruce, 1979].

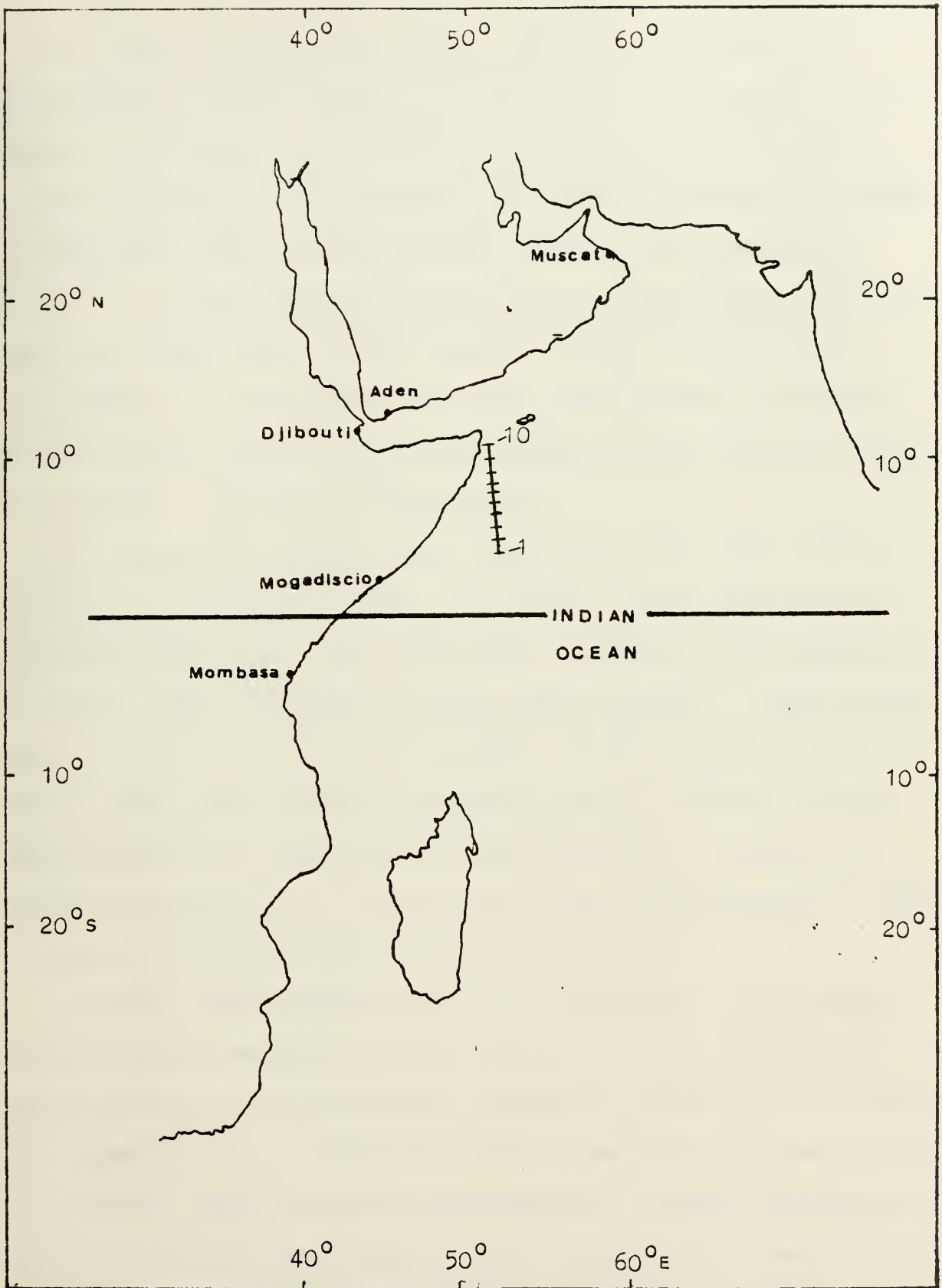

Figure 23. USNS KINGSPORT track and XBT profile locations (-).

The ICAPS program was used to convert the thermal data to sound speed profiles (SSP). Two SSP's were generated at each station; one based on the observed data and the other based on the climatology from ICAPS. The ICAPS climatology is based on quarterly averages representing rather large geographic areas. Along the summer track only four ICAPS climatological profiles (ICAPS water masses) exist. These climatological water masses do not reveal the eddy field actually observed. For the winter track, two climatological water masses are used to represent the area of observation.

The resulting profiles were inserted in the FACT (Fast Asymptotic Coherent Transmission) model for the computation of propagation loss. The FACT model assumes a flat bottom and a single, range independent sound speed profile. (The assumption of a flat bottom is not harmful in this study since the bottom along both tracks is generally flat. However, range independence is a compromising approximation.) Propagation loss is calculated as a function of range and frequency. FACT is based on classic ray theory.

The data were examined for two situations: 1) a towed array at 100 m sensing a signal at 100 Hz; and, 2) a hull mounted sonar at 10 m sensing a signal at 2000 Hz. The signal was hypothesized to originate from a transitting submarine at 100 m depth. Each situation was modeled to study propagation conditions during summer and winter. Direct path ranges were calculated using FOM's (Figure of Merit) of 90, 100 and 110 dB

at 100 Hz and 80, 90 and 100 dB at 2000 Hz. Bottom loss calculations were computed using a bottom type four for 100 Hz and bottom type five for 2000 Hz. These values are representative of the area and taken from the ASW Prediction Area charts.

The accuracy of prediction was calculated as the percent difference in direct path range between that computed from climatology and that computed using the observed thermal structure:

$$\% \text{ Accuracy} = \frac{\text{Climatology - Observed}}{\text{Observed}}$$

For each FOM the accuracy was determined and assigned a positive value if climatology provided an overprediction and a minus value if climatology provided an underprediction of range. The range predictions based upon the observed data were assumed to be accurate. No attempt was made to ascertain the validity of the FACT model itself.

B. RESULTS

1. Summer Monsoon (100 Hz)

a. Within Eddies

Sound speed profiles from Stations B, E, I and K were selected to represent conditions within the confines of the warm core eddies (Figures 22 and 24). Stations I and K were represented by one climatological water mass while Stations B and E were represented by two different historical profiles. Source and receiver depths were below the layer

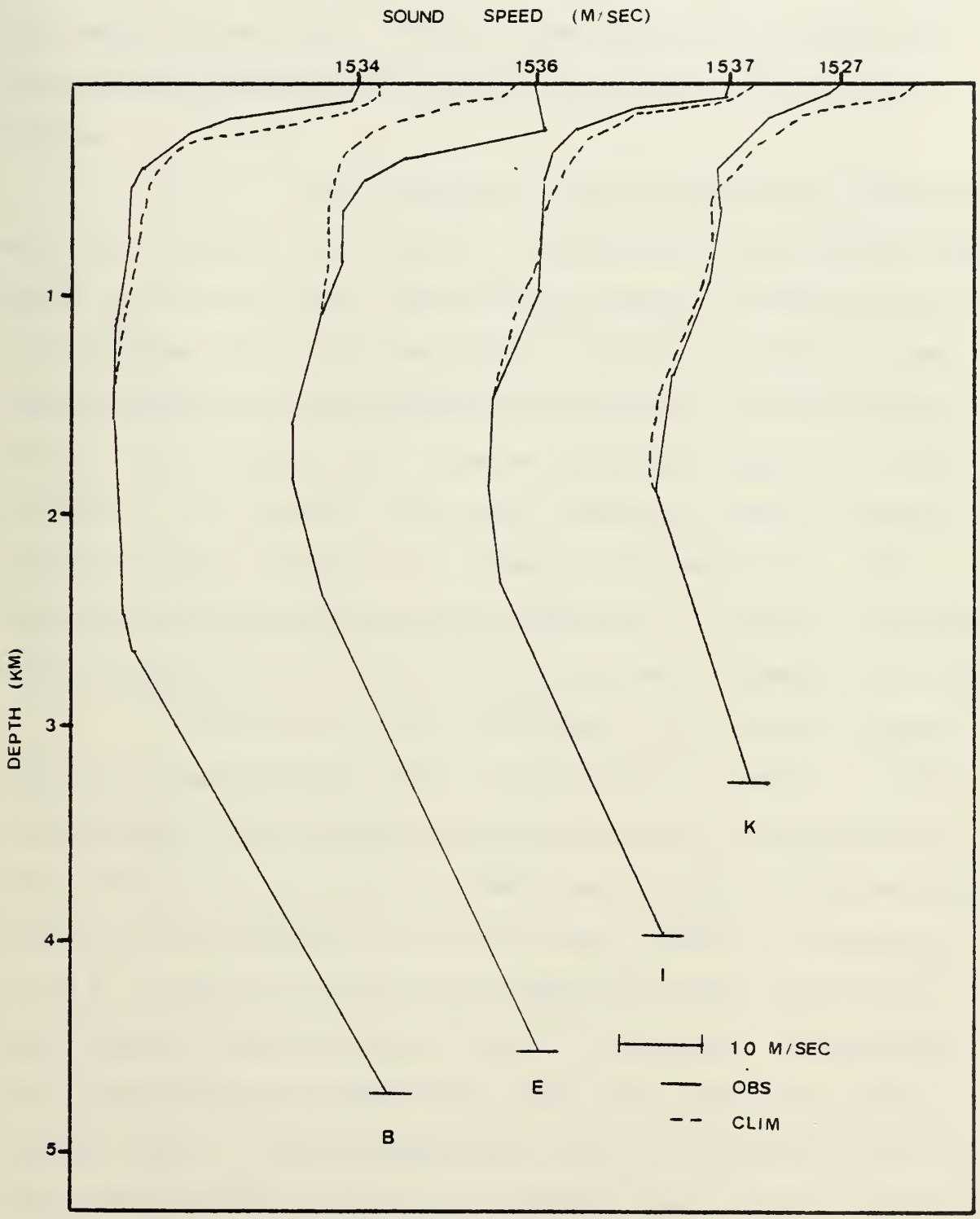

Figure 24. Sound speed profiles within warm core eddies, August 1976.

at Stations B, I and K, but at Station E, in the center of the main warm core eddy, source and receiver were both within the deep surface duct. Table I summarizes range predictions and accuracy results for stations located within the warm eddies.

For a FOM of 90 dB the accuracy was not exceptionally good except at Station K. At Station B the observed range was much less than the climatological range. Examination of the observed and historical SSP at Station B reveals a less severe gradient in the thermocline region of the historical profile which results in a greater predicted range for this situation. At Station I the good channeling seen in the observed profile resulted in a greater observed range. The accuracy of the climatological prediction at Station K resulted from the similarity of the profile gradients beneath the layer.

At Station E the historical SSP does not reveal the strong surface duct seen in the observed profile. Thus, the observed range was much greater than the climatological prediction and two to three times greater than the below layer conditions experienced in the shallower eddies at Stations B, I and K. Figure 25 shows the transmission loss curves for the observed and climatological data at Station E. The observed loss curve falls off much more slowly than does the climatological curve. The intersection of the 90 dB FOM with the TL curve thus takes place at much greater range for the observed data than it does for the historical data.

TABLE I

COMPARISON OF ACOUSTIC RESULTS AT 100 Hz
DURING SUMMER FOR STATIONS WITHIN EDDIES

FOM (dB)	RANGE (Obs/Clim) (kyds)	ACCURACY (%)
	Station B	
90	10/16	+60
100	69/79	+14
110	-	-
	Station E	
90	31/9	-71
100	75/76	+1
110	-	-
	Station I	
90	16/11	-31
100	66/58	-12
110	126/110	-13
	Station K	
90	12/13	+8
100	58/44	-24
110	111/84	-24

- MDR exceeds program computational limits.

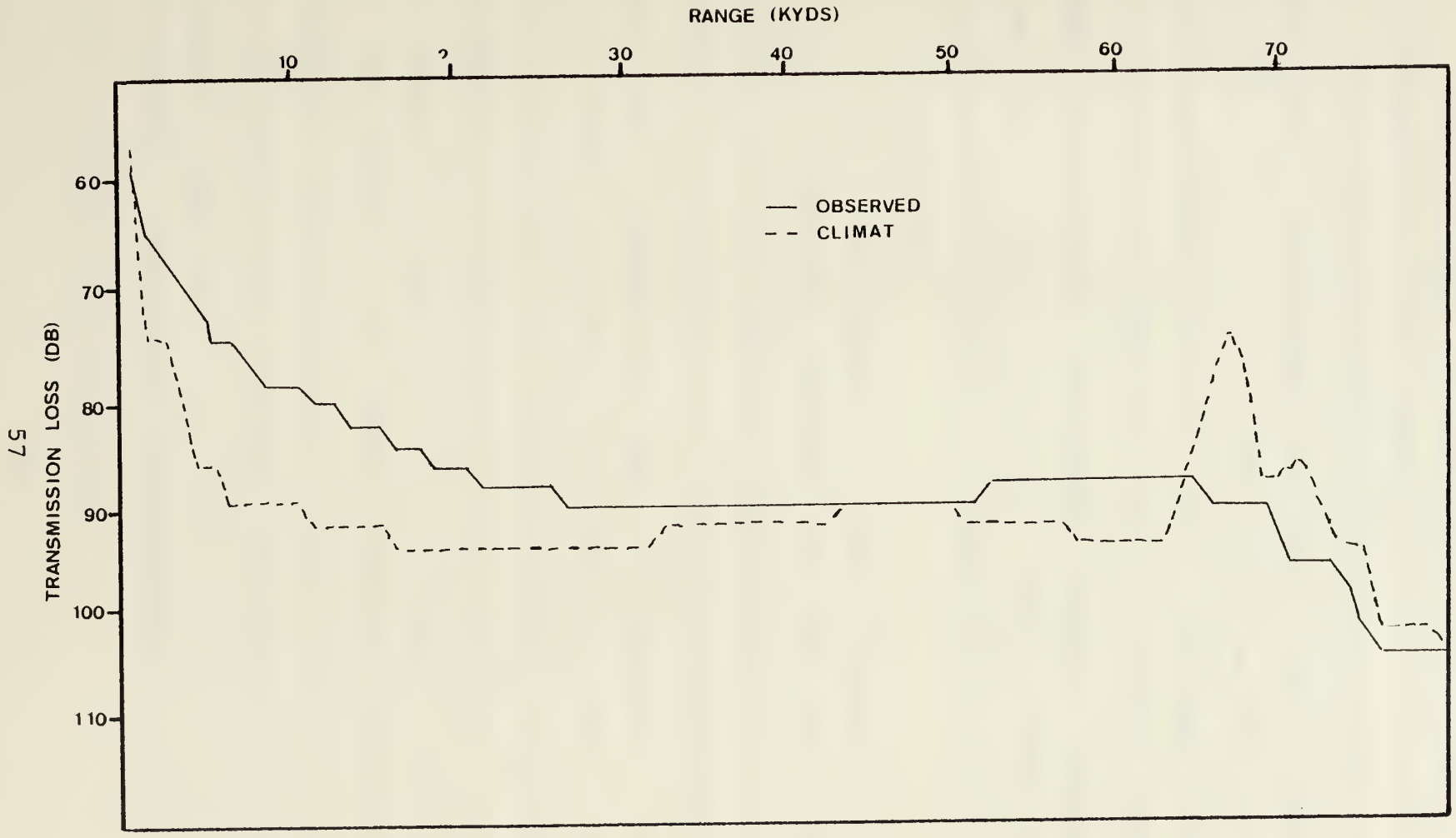

Figure 25. Transmission loss curves for Station E. Source at 100 m, receiver at 100 m, 100 Hz.

At the higher FOM's, accuracy was much improved. Note the similarity of the TL curves in Figure 25 at extended range. CZ propagation was observed at Stations B and I and was predicted by climatological profiles to occur at Stations B and E. At Station B four CZ peaks were observed and two CZ peaks were predicted by historical data. The ranges of the two climatological CZ peaks were within five percent of the two middle peaks observed. The shorter ranges at Stations I and K were due to bottom interactions. Figure 24 shows that these stations are significantly shallower than B and E.

b. Eddy Edge

SSP's from Stations A, C and G (Figures 22 and 26) were chosen to represent conditions within but near the edge of the warm core eddies where the thermocline begins to shoal. Each station was represented by a different climatological profile. Table II summarizes ranges and accuracies for these stations. Source and receiver were below the layer at each station. At Stations A and C observed ranges were less than those predicted by climatology for an FOM of 90 dB. It is not readily apparent why there was such a difference in predicted ranges, but perhaps the less severe thermocline gradient of the historical profile permitted a greater range to be predicted. At Station G the historical SSP resulted in an underprediction of range because the channeling effects of the observed profile, not present in the historical profile, resulted in greater forecasted ranges.

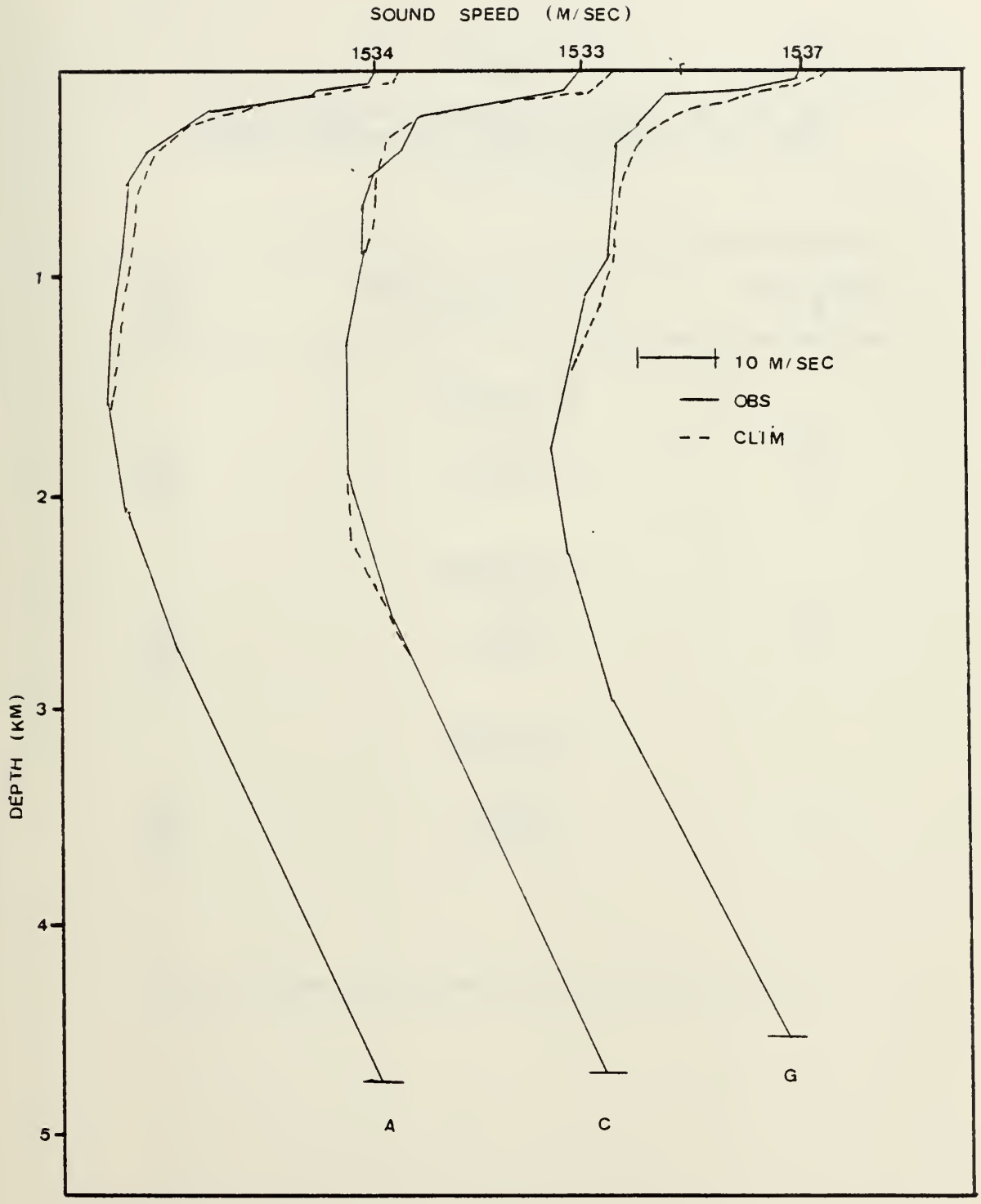

Figure 26. Sound speed profiles near the edge of the eddy, August 1976.

TABLE II

COMPARISON OF ACOUSTIC RESULTS AT 100 Hz DURING SUMMER FOR STATIONS NEAR THE EDGE OF WARM EDDIES

FOM (dB)	RANGE (Obs/Clim) (kyds)	ACCURACY (%)
	Station A	
90	12/15	+25
100	80/76	-5
110	-	-
	Station C	
90	9/16	+77
100	80/79	-1
110	-	-
	Station G	
90	12/11	-8
100	69/71	+2
110	162/150	-7

- MDR exceeds program computational limits.

As in the eddy stations, accuracy was much improved at the higher FOM's. Figure 27 shows the transmission loss curves for Station C. Again, as at Station E within the warm core eddy, note the similarity of the TL curves at extended ranges.

CZ propagation was observed at all three stations and predicted by the climatology to occur at all three. Accuracy was exceptional at Station A. Three CZ's were predicted by the historical data and three were predicted by the observed data. Range differences between the two predictions were less than 4.5%. Climatology underpredicted in each case.

At Station C three CZ's were also predicted from historical and observed data, with an accuracy of better than 1.5%. At Station G two CZ's were predicted from historical data and three from observed data. The accuracies of the predictions were again good, within 4.5%.

c. Upwelling Areas

Stations D, F, H and J are representative of areas located in cold upwelling areas between the warm core eddies (Figure 22). SSP's from these stations are shown in Figure 28. Station D was represented by a different historical profile than the other stations. Table III summarizes predicted ranges and accuracies for these stations within upwelling areas. Source and receiver were beneath the mixed layer at all of these stations.

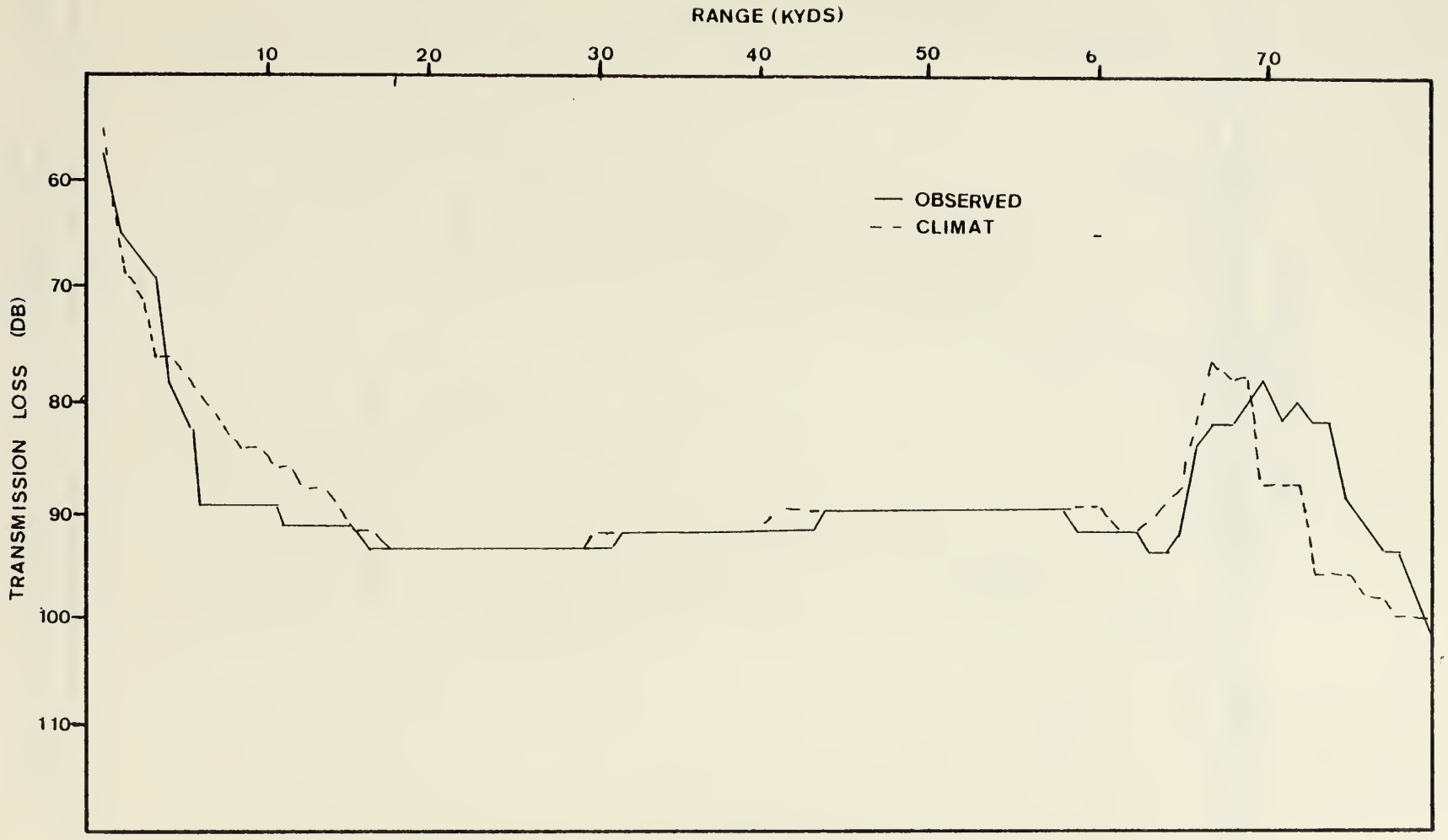

Figure 27. Transmission loss curves for Station C.
Source at 100 m, receiver at 100 m, 100 Hz.

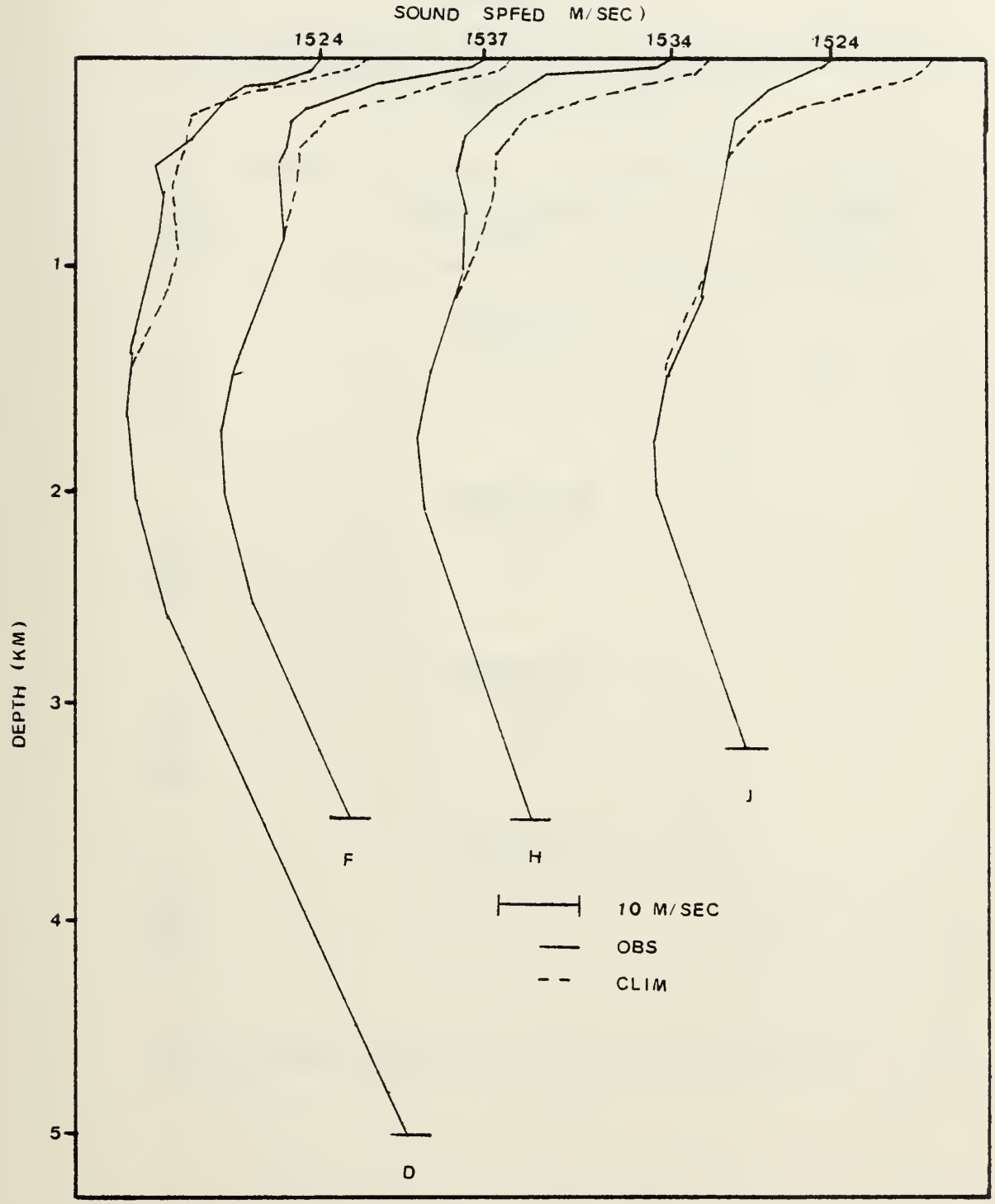

Figure 28. Sound speed profiles in upwelling areas, August 1976.

TABLE III

COMPARISON OF ACOUSTIC RESULTS AT 100 Hz
DURING SUMMER FOR STATIONS
IN UPWELLING AREAS

FOM (dB)	RANGE (Obs/Clim) (kyds)	ACCURACY (%)
	Station D	
90	59/74	+25
100	-	-
110	-	-
	Station F	
90	114/134	+17
100	-	-
110	-	-
	Station H	
90	84/88	+4
100	-	-
110	-	-
	Station J	
90	86/80	-7
100	-	-
110	-	-

- MDR exceeds program computational limits.

For an FOM of 90 dB, climatology overpredicted the direct path range at Stations D, F and H due to the less severe gradient of the climatological profile, and more importantly, due to the channeling effect of the upper 1000 m. Ranges at these stations were three to four times greater than at the other stations within the warm eddies because of this channeling. At Station J the observed gradient was less severe than the climatological profile and thus, climatology underpredicted the range. Only slight channeling was evident in the upper 1000 m at Station J. At higher FOM's all ranges exceeded the program limits. However, as in previous cases, transmission loss curves are similar at extended ranges. Figure 29 shows a comparison of the TL curves based on the SSP's from Station H.

CZ propagation was observed at Stations D and H but predicted by climatology to occur only at Station D. The decrease in transmission loss apparent at 40 and 80 kyds on the climatological TL curve for Station H (Figure 29) was not attributable to CZ since no depth excess existed in the historical SSP (Figure 28). This dB gain must be attributed to bottom bounce. Climatology predicted two CZ peaks at Station D; three were observed. Accuracy was good, less than 1.5% difference in range. Climatology did not predict the initial CZ peak which was observed at 64 kyds.

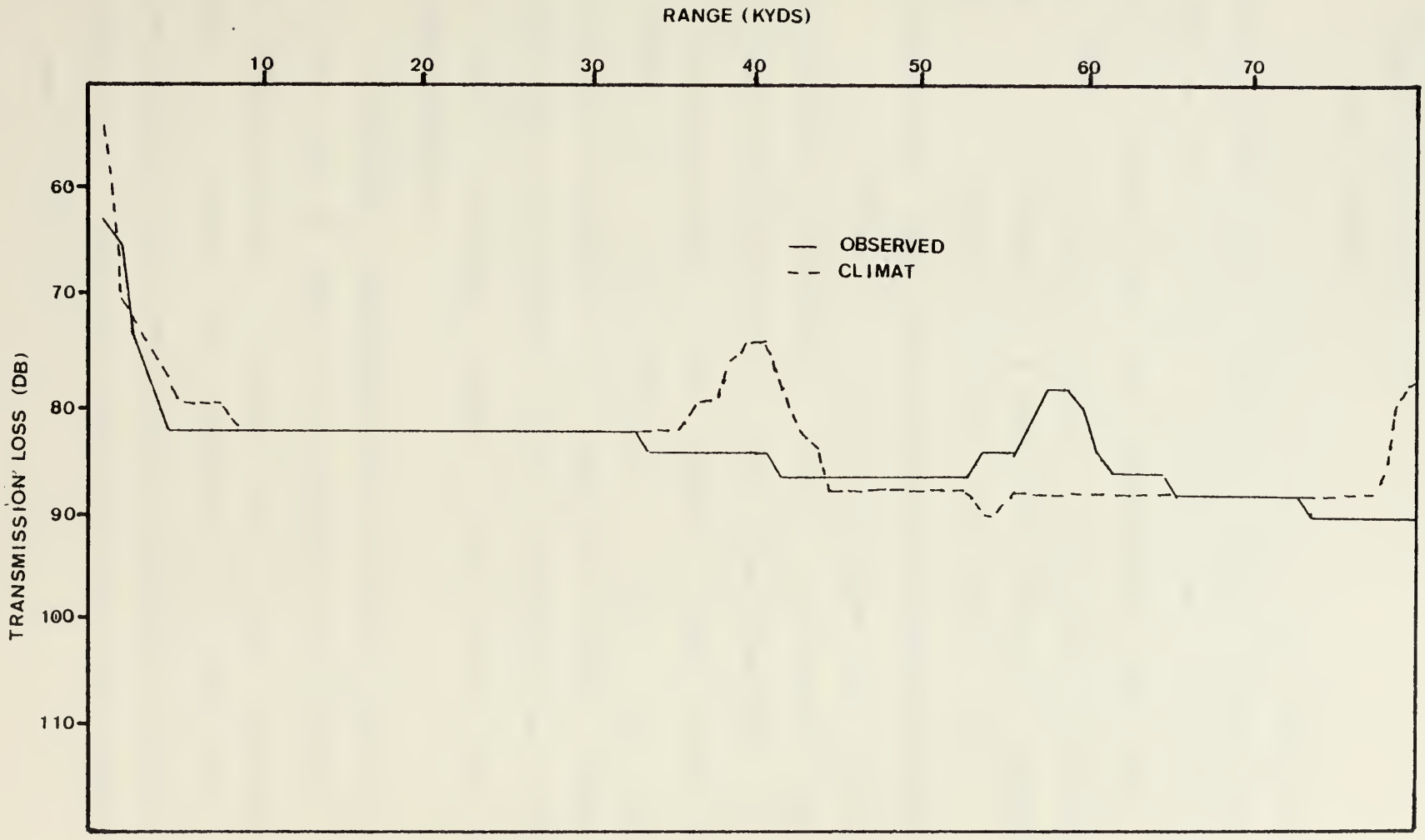

Figure 29. Transmission loss curves for Station H.
Source at 100 m, receiver at 100 m, 100 Hz.

2. Summer Monsoon (2000 Hz)

a. Within Eddies

As before, Stations B, E, I and K were found within the confines of the warm core eddies. Figure 24 depicts the SSP's from these four stations. Station B was represented by one historical SSP and the other three stations were represented by one climatological profile. Transmission was across the layer at all stations but E where the principal transmission path was via ducting within the deep surface layer. Table IV summarizes ranges and accuracies at these stations.

At an FOM of 80 dB predicted ranges were short and generally accurate at Stations B, I and K. At Station E the observed range was significantly (60%) longer than that predicted by climatology due to the trapping of sound in the deep (175 m) surface duct. As at Stations B, I and K, cross layer transmission was indicated by the historical SSP for Station E. To some extent the observed range at Station E was probably limited by surface scattering caused by the high seas and winds of the summer monsoon.

Climatology underpredicted the actual range at Stations B and I for an FOM of 90 dB because the gradient in the upper thermocline was more severe than in the climatological profile. At Station E the presence of the deep duct in the observed profile led to an extreme difference in the predicted ranges, i.e., the actual range was four times greater than that based on archival data.

TABLE IV

COMPARISON OF ACOUSTIC RESULTS AT 2000 Hz
DURING SUMMER FOR STATIONS WITHIN EDDIES

FOM (dB)	RANGE (Obs/Clim) (kyds)	ACCURACY (%)
	Station B	
80	5/6	+20
90	13/8	-38
100	27/29	+7
	Station E	
80	10/4	-60
90	23/6	-74
100	40/27	-32
	Station I	
80	7/6	-14
90	13/8	-38
100	33/30	-9
	Station K	
80	6/6	0
90	8/8	0
100	38/40	+5

For an FOM of 100 dB the accuracy was good (within 10%) for all stations but E. Here again, the absence of the strong surface duct in the climatological profile caused a severe shortening of the expected range. Figure 30 shows TL curves for Station E. The observed TL curve did not drop as quickly as did the climatological curve. At FOM's greater than 100 dB, the accuracy would improve due to the similarity of the TL curves at extended range.

b. Eddy Edge

As before, Stations, A, C and G (Figures 22 and 26) were located near the edge of an eddy at a point where the thermocline had begun to shoal. Transmission was cross-layer at each of these stations. Table V summarizes ranges and accuracies at these stations.

Accuracy at all FOM's was generally good, within one to two kyds, although the percent error appeared large due to the relatively short ranges involved. An examination of the SSP's revealed a marked similarity between the observed and historical profiles. Figure 31 shows TL curves from Station C. The curves are remarkably similar at close range. CZ propagation was observed at Stations A and C while climatology predicted that CZ propagation was not possible at these stations. Depth excess did not exist at Station G nor was it expected from the historical SSP.

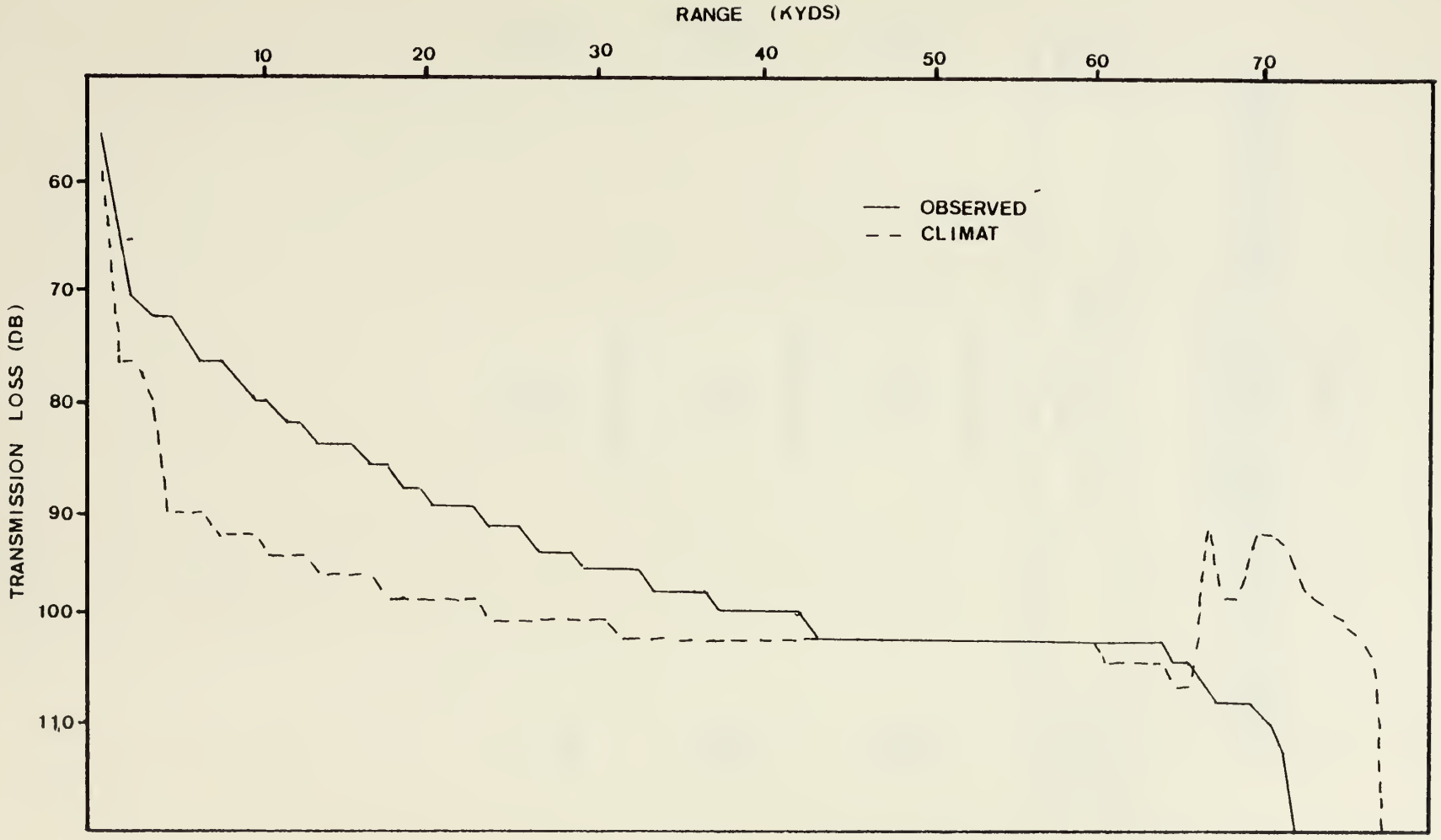

Figure 30. Transmission loss curves for Station E.
Source at 100 m, receiver at 10 m, 2000 Hz.

TABLE V

COMPARISON OF ACOUSTIC RESULTS AT 2000 Hz
DURING SUMMER FOR STATIONS NEAR THE EDGE
OF WARM EDDIES

FOM (dB)	RANGE (Obs/Clim) (kyds)	ACCURACY (%)
	Station A	
80	6/7	+17
90	10/8	-20
100	27/28	+4
	Station C	
80	5/7	+40
90	5/8	+60
100	27/29	+7
	Station G	
80	5/6	+20
90	8/8	0
100	18/17	-5

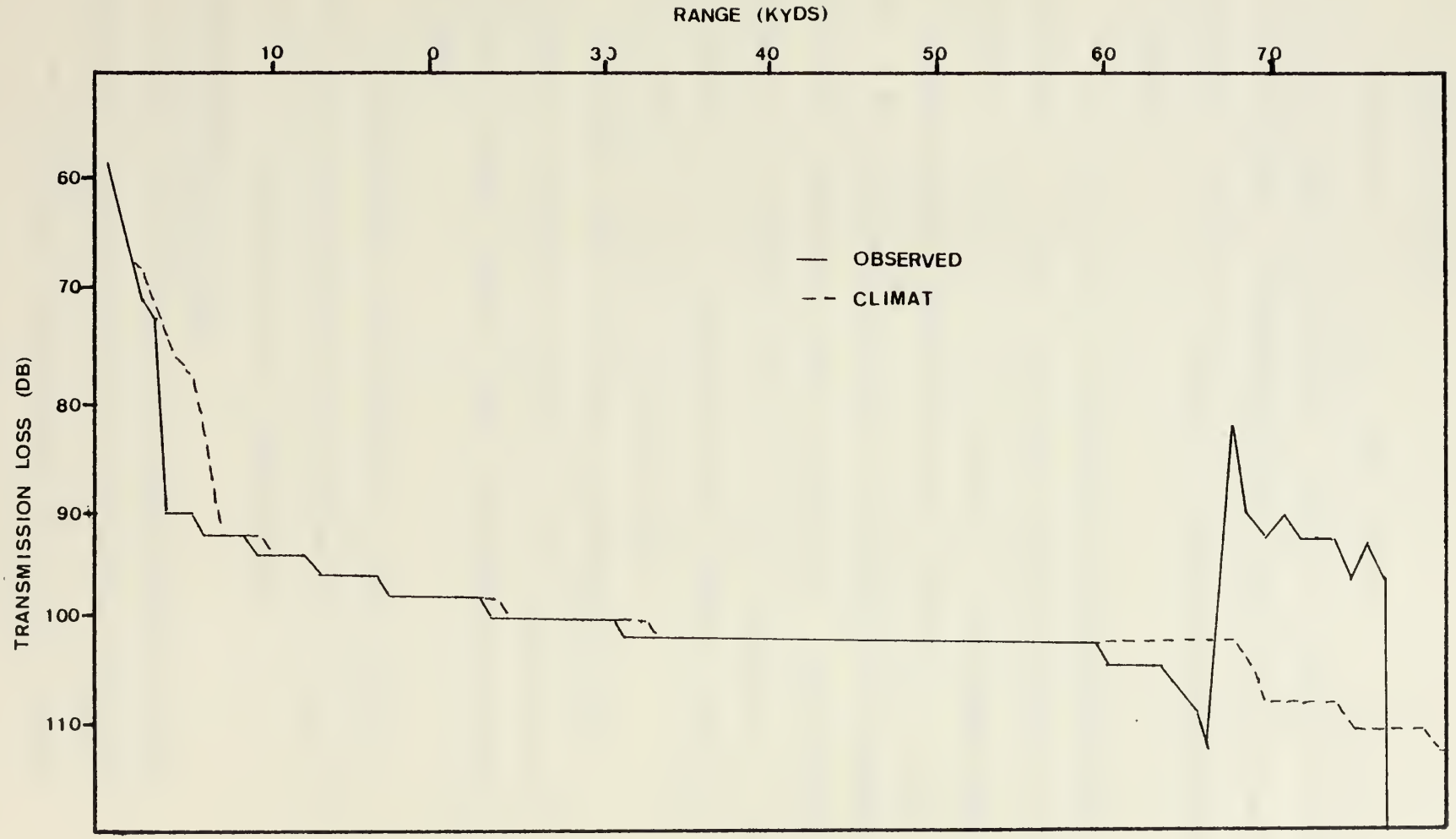

Figure 31. Transmission loss curves for Station C.
Source at 100 m, receiver at 10 m, 2000 Hz.

c. Upwelling Areas

Stations D, F, H and J were located in the upwelling areas between the warm core eddies. Figure 28 depicts the SSP's at these four stations. Transmission was cross-layer at each of these stations. Table VI summarizes ranges and accuracies at these stations.

At an FOM of 80 dB climatology overpredicted the range at Stations F, G and I. The less severe gradient of the historical SSP in the upper layer caused its predicted range to be two to three times greater than that indicated by the observed SSP. The archival data did not adequately represent conditions in this region of active upwelling. The historical SSP at Station D was different than that for Stations F, H and I. Here, (Station D), the historical and observed profiles were similar and the accuracy was quite good.

At higher FOM's accuracy was generally good. Figure 32 shows TL curves for Station H. The similarity of the TL curves at longer ranges causes the greater accuracy at the higher FOM's.

CZ propagation was observed at only Station D. The archival data also predicted CZ propagation at Station D. The accuracy of the prediction was within 2.2%.

3. Winter Monsoon (100 Hz)

The thermal field during the winter monsoon season was represented by the ten XBT drops of the USNS KINGSPORT (Figure 23). No prominent features such as an eddy field

TABLE VI

COMPARISON OF ACOUSTIC RESULTS AT 2000 Hz
DURING SUMMER IN UPWELLING AREAS

FOM (dB)	RANGE (Obs/Clim) (kyds)	ACCURACY (%)
	Station D	
80	6/5	-16
90	14/15	+7
100	50/53	+6
	Station F	
80	3/7	+130
90	33/37	+12
100	42/51	+21
	Station H	
80	4/6	+50
90	23/22	-4
100	44/48	+9
	Station J	
80	2/6	+200
90	24/23	-4
100	50/44	-12

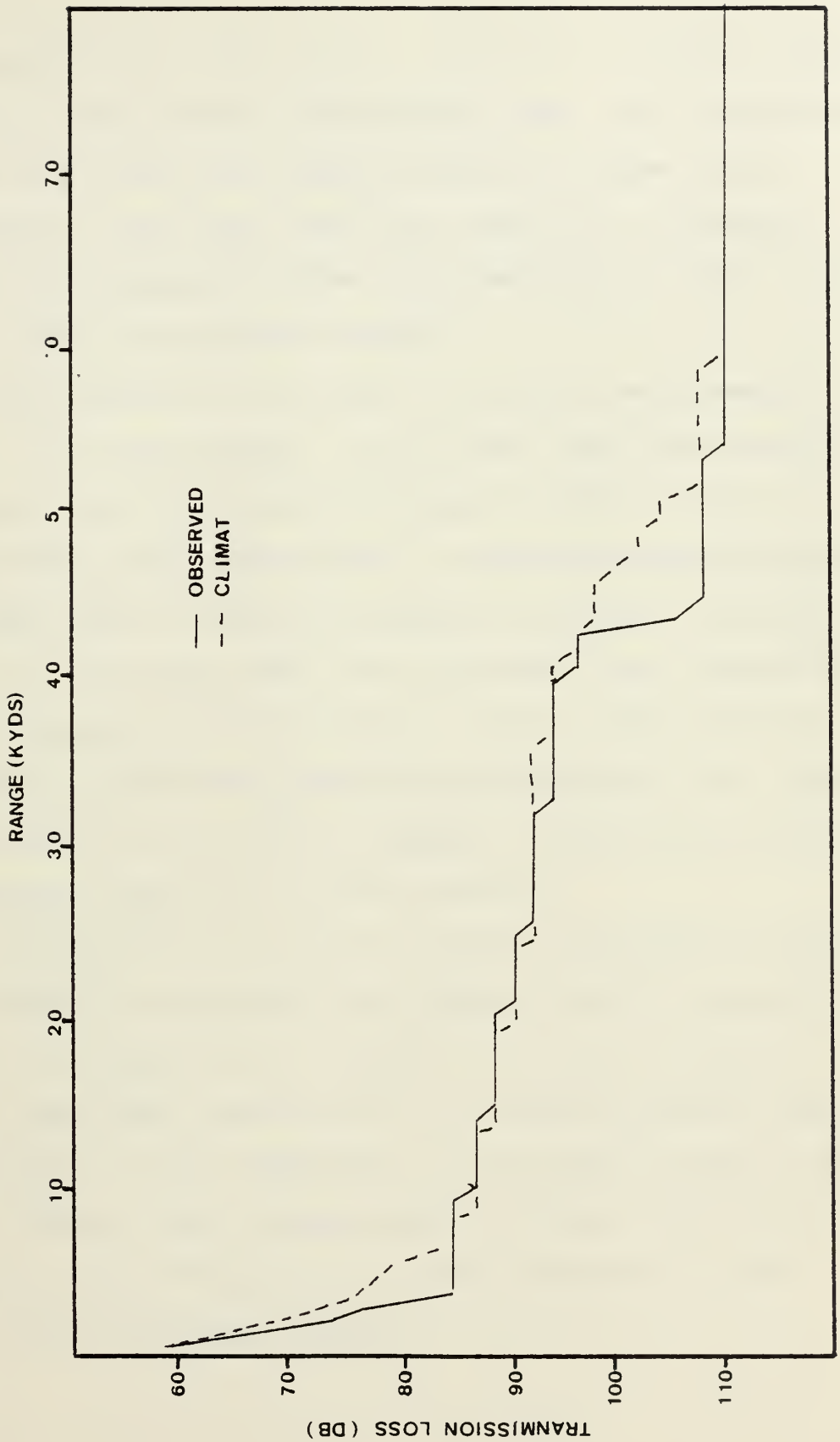

Figure 32. Transmission loss curves for Station H. Source at 100 m, receiver at 10 m, 2000 Hz.

were observed during this season. Stations 2 through 10 were represented by one ICAPS climatological SSP. All transmission paths were for source and receiver below the mixed layer. A depth excess of less than 1000 m was observed at Stations 2 through 8, thus permitting some CZ propagation to occur. All historical SSP's were bottom limited.

The results of the acoustic analysis are presented in Table VII. At each station, for all FOM's the climatological range grossly underpredicted the range forecasted from the observed SSP's. All observed SSP's revealed intense channeling in the upper 1000 m (see, for example, the SSP for Station 2, Figure 33). Historical SSP's did not reveal this channeling and thus predicted severely shorter ranges. Some of the ten observed SSP's exhibited considerable complexity (e.g., Station 10, Figure 33) but this did not appear to appreciably influence the forecasted ranges or relative accuracy.

Figures 34 and 35 show TL curves at Stations 2 and 10. Both TL curves for observed data showed an initial rapid loss and then a leveling out at a range of less than 10 kyds. On the other hand, the climatological TL curves revealed bottom interactions at 15 kyd increments. A CZ peak is noted at 70 kyds for Station 2 but the peak seen at 50 kyds for Station 10 is probably due to focusing by bottom reflections as the Station 10 SSP is bottom limited.

TABLE VII

COMPARISON OF ACOUSTIC RESULTS AT 100 Hz
DURING WINTER

FOM (dB)	RANGE (Obs/Clim) (kyds)	ACCURACY (%)	FOM (dB)	RANGE (Obs/Clim) (kyds)	ACCURACY (%)
	Station 1			Station 6	
90	63/33	-47	90	83/38	-54
100	42/71	-23	100	174/75	-57
110	-	-	110	-	-
	Station 2			Station 7	
90	66/38	-42	90	64/38	-41
100	162/75	-54	100	152/75	-51
110	-	-	110	-	-
	Station 3			Station 8	
90	79/38	-52	90	66/38	-42
100	182/75	-59	100	166/75	-45
110	-	-	110	-	-
	Station 4			Station 9	
90	80/38	-52	90	64/36	-48
100	170/75	-54	100	188/70	-63
110	-	-	110	-	-
	Station 5			Station 10	
90	79/38	-52	90	52/36	-31
100	152/75	-51	100	153/68	-56
110	-	-	110	-	-

- MDR exceeds program computational limits.

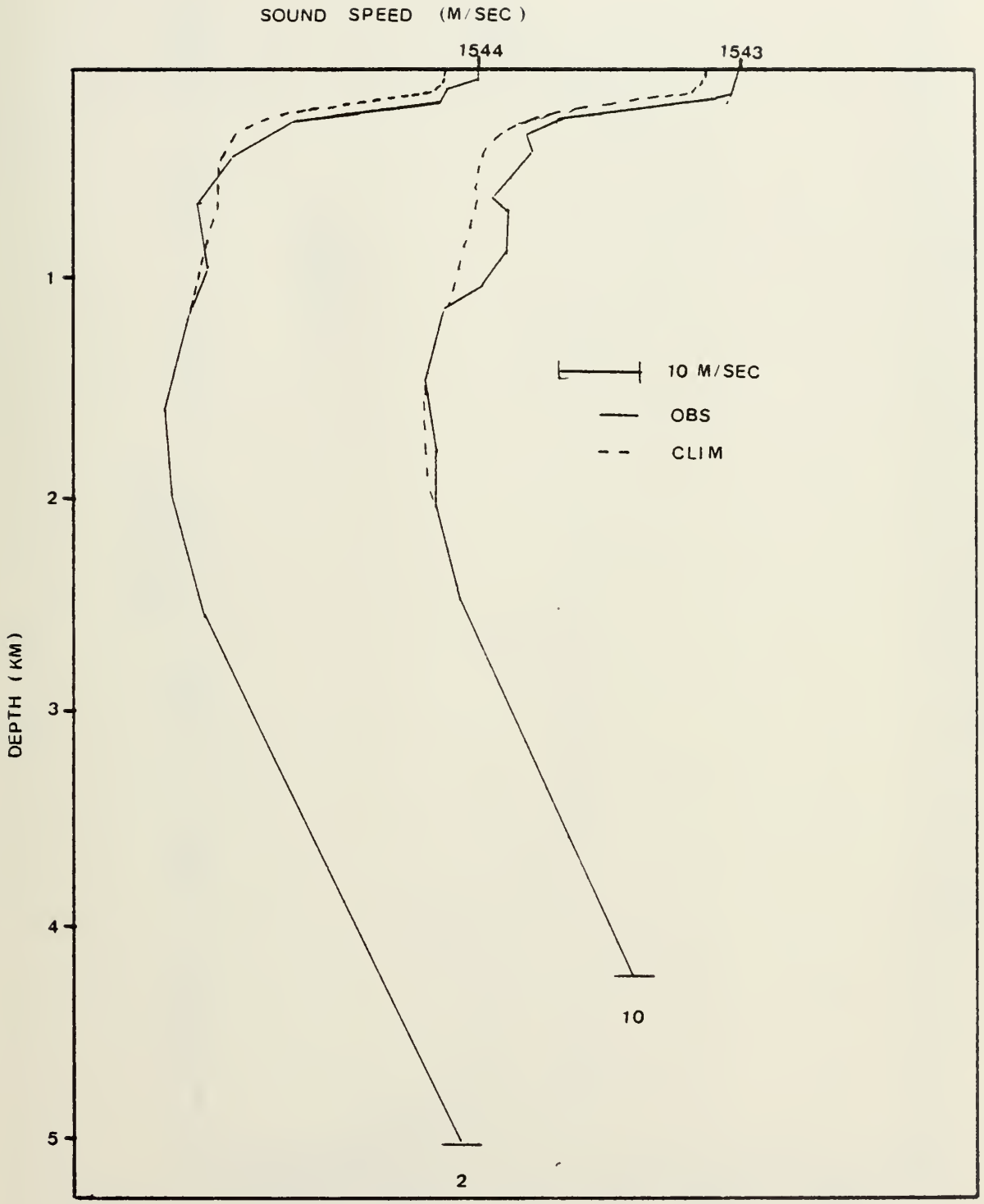

Figure 33. Sound speed profile at Stations 2 and 10, March 1977.

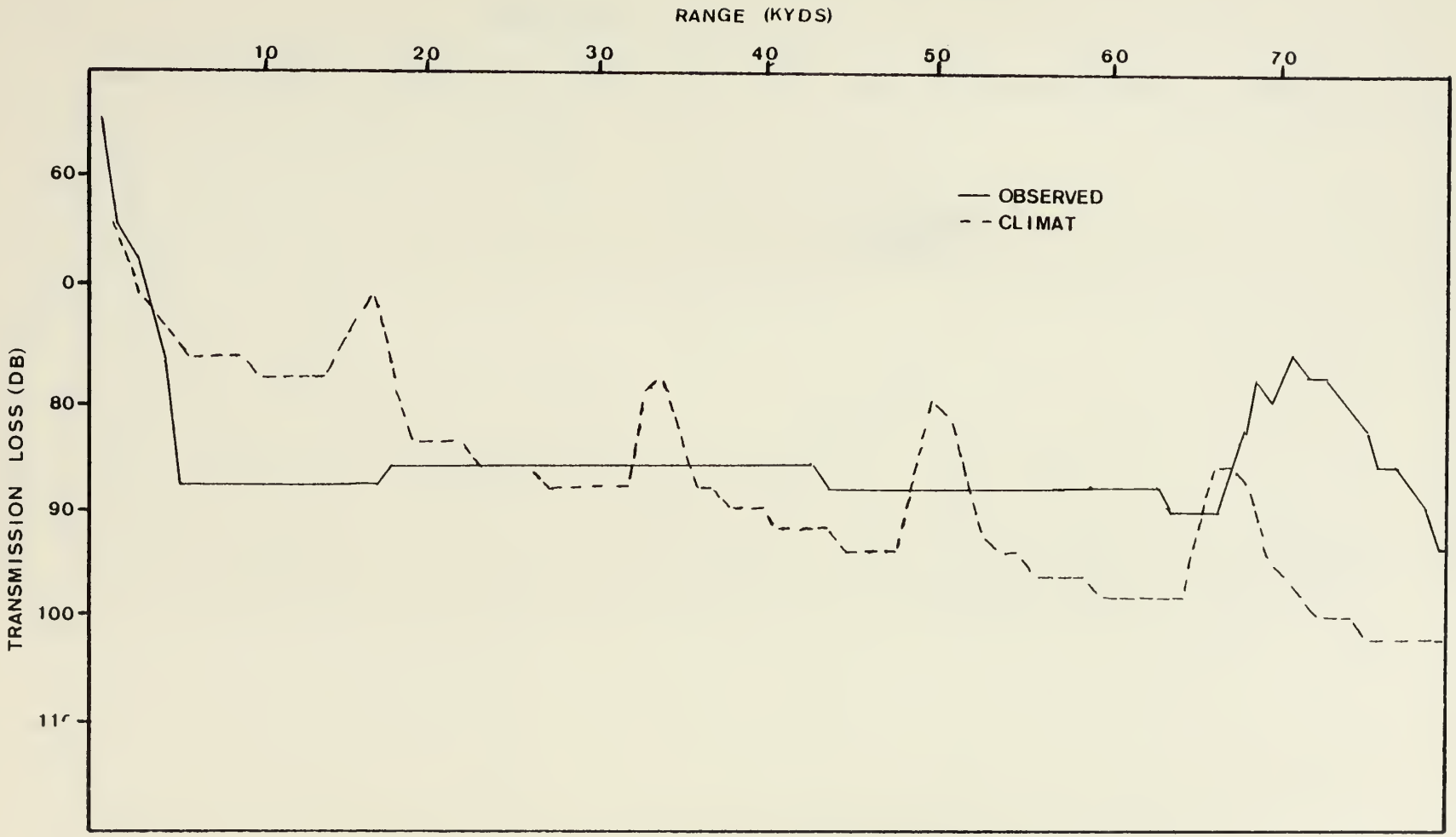

Figure 34. Transmission loss curves for Station 2. Source at 100 m, receiver at 100 m, 100 Hz.

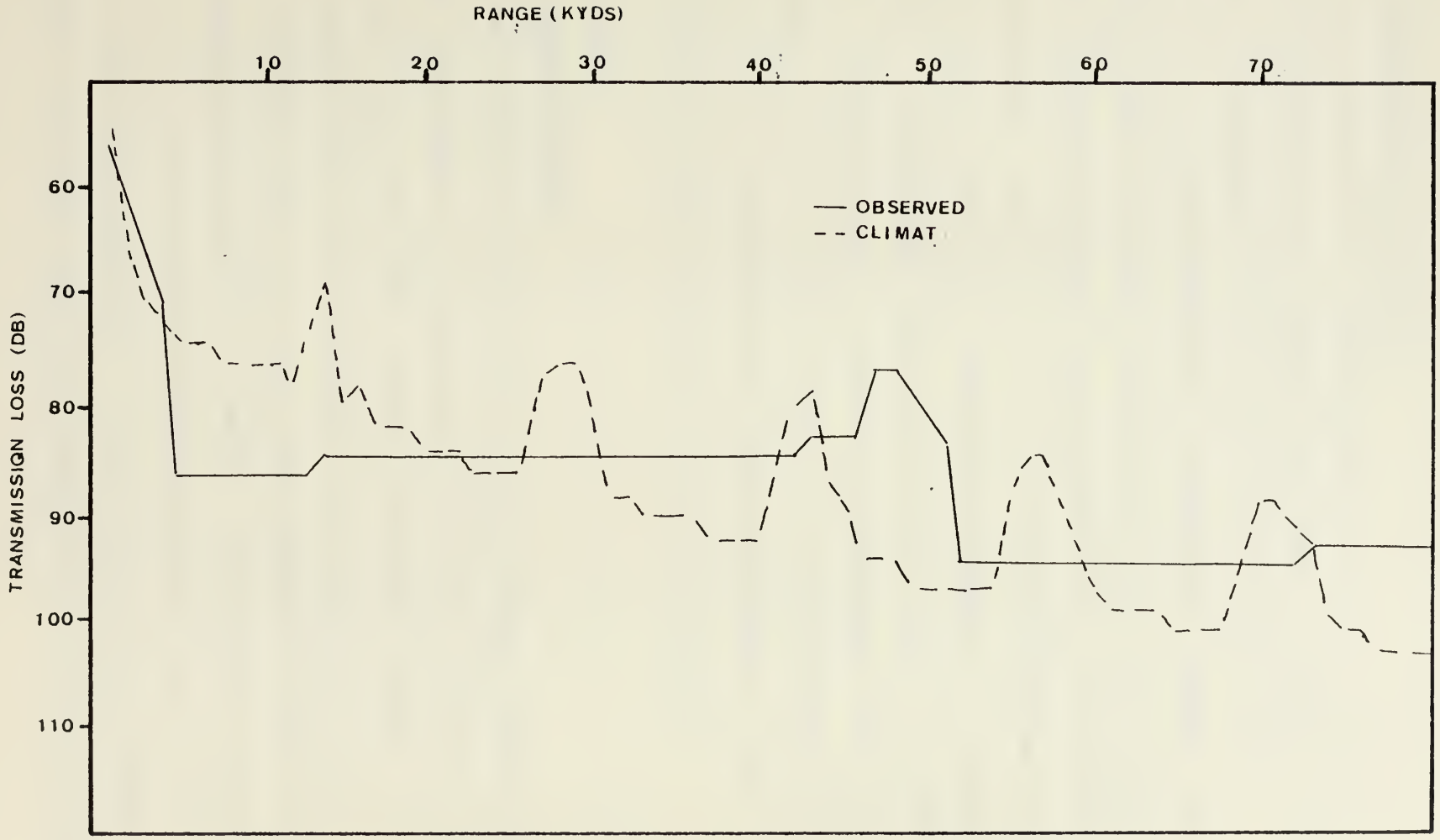

Figure 35. Transmission loss curves for Station 10.
Source at 100 m, receiver at 100 m, 100 Hz.

4. Winter Monsoon (2000 Hz)

As in the previous winter case for 100 Hz, accuracies were extremely poor at all stations and FOM's. The poor representation of the sound field by the climatological data is reflected in the marked difference in predicted ranges. All transmission paths for source and receiver were cross-layer. Table VIII summarizes ranges and accuracies for all stations during the winter. At FOM's of 80 and 90 dB climatology overpredicted the range due to a less severe gradient in the upper thermocline. Climatology underpredicted the range at an FOM of 100 dB. Figures 36 and 37 show TL at Stations 2 and 10, respectively. The TL curves intersect at approximately 20 kyds and 92 dB as the observed TL curve flattened and the climatological TL curve continued to fall off rapidly.

C. DISCUSSION

1. Summer Monsoon

Low frequency towed arrays in the western Indian Ocean main warm core eddy will experience conditions similar to those found in the large warm core eddies of the Gulf Stream. A strong surface duct allows extremely long detection ranges. ICAPS climatology does not reveal this prominent feature and thus severely underpredicts the range. The smaller warm core eddies do not extend to great depth and thus are not as conducive to long range detection. Within these smaller eddies transmission paths for source and receiver are below the mixed layer.

TABLE VIII

COMPARISON OF ACOUSTIC RESULTS AT 2000 Hz
DURING SUMMER

FOM (dB)	RANGE (Obs/Clim) (kyds)	ACCURACY (%)	FOM (dB)	RANGE (Obs/Clim) (kyds)	ACCURACY (%)
80	Station 1			Station 6	
80	3/5	+66	80	5/6	+20
90	13/16	+23	90	8/20	+150
100	47/26	-45	100	64/29	-55
	Station 2			Station 7	
80	4/6	+50	80	4/6	+50
90	9/20	+120	90	8/20	+150
100	52/29	-44	100	46/29	-37
	Station 3			Station 8	
80	4/6	+50	80	4/6	+50
90	9/20	+120	90	8/20	+150
100	56/29	-48	100	46/29	-37
	Station 4			Station 9	
80	4/6	+50	80	4/6	+50
90	8/20	+150	90	11/19	+72
100	64/29	-55	100	60/29	-53
	Station 5			Station 10	
80	4/6	+50	80	3/6	+100
90	8/20	+150	90	12/18	+58
100	50/29	-55	100	50/27	-46

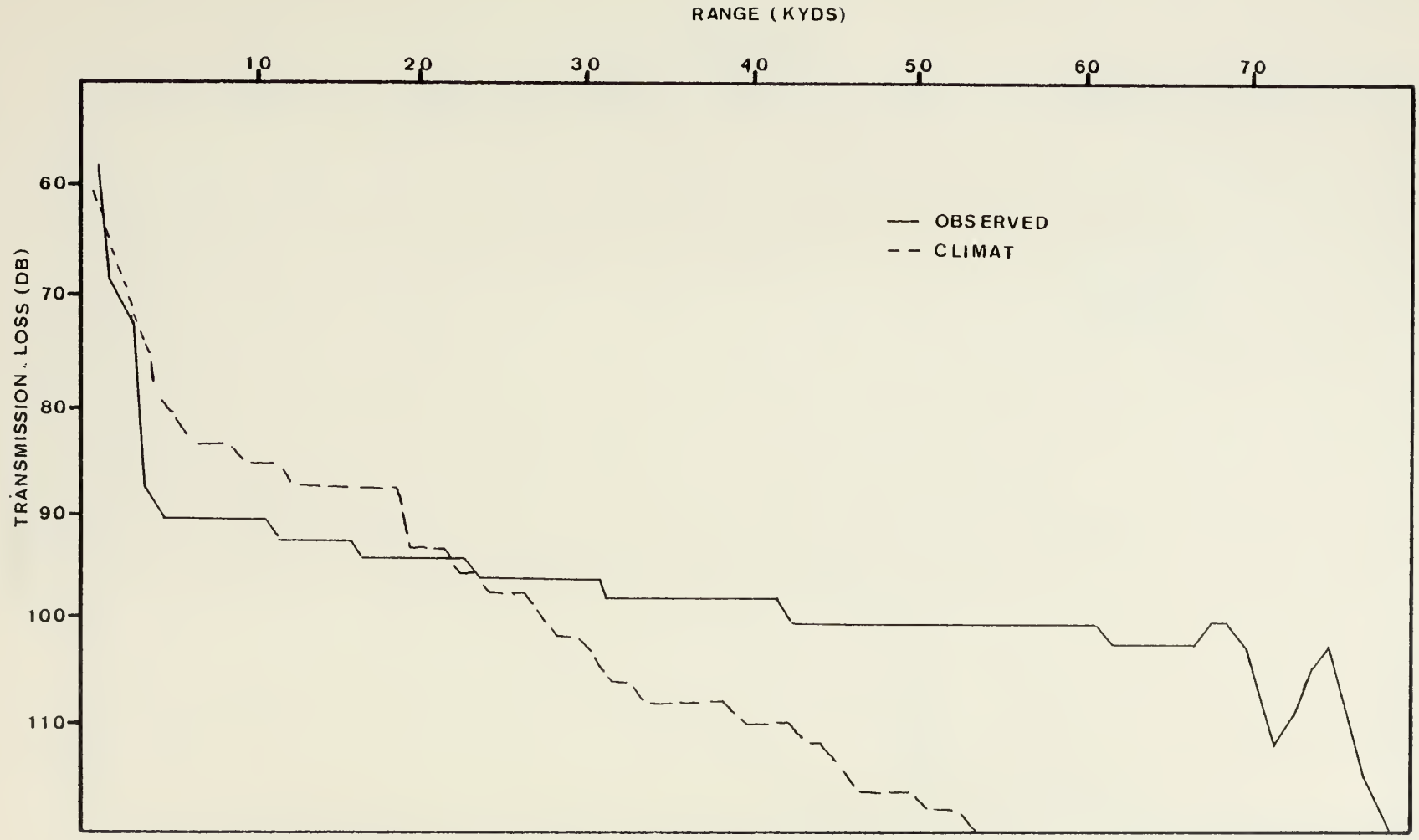

Figure 36. Transmission loss curves for Station 2.
Source at 100 m, receiver at 10 m, 2000 Hz.

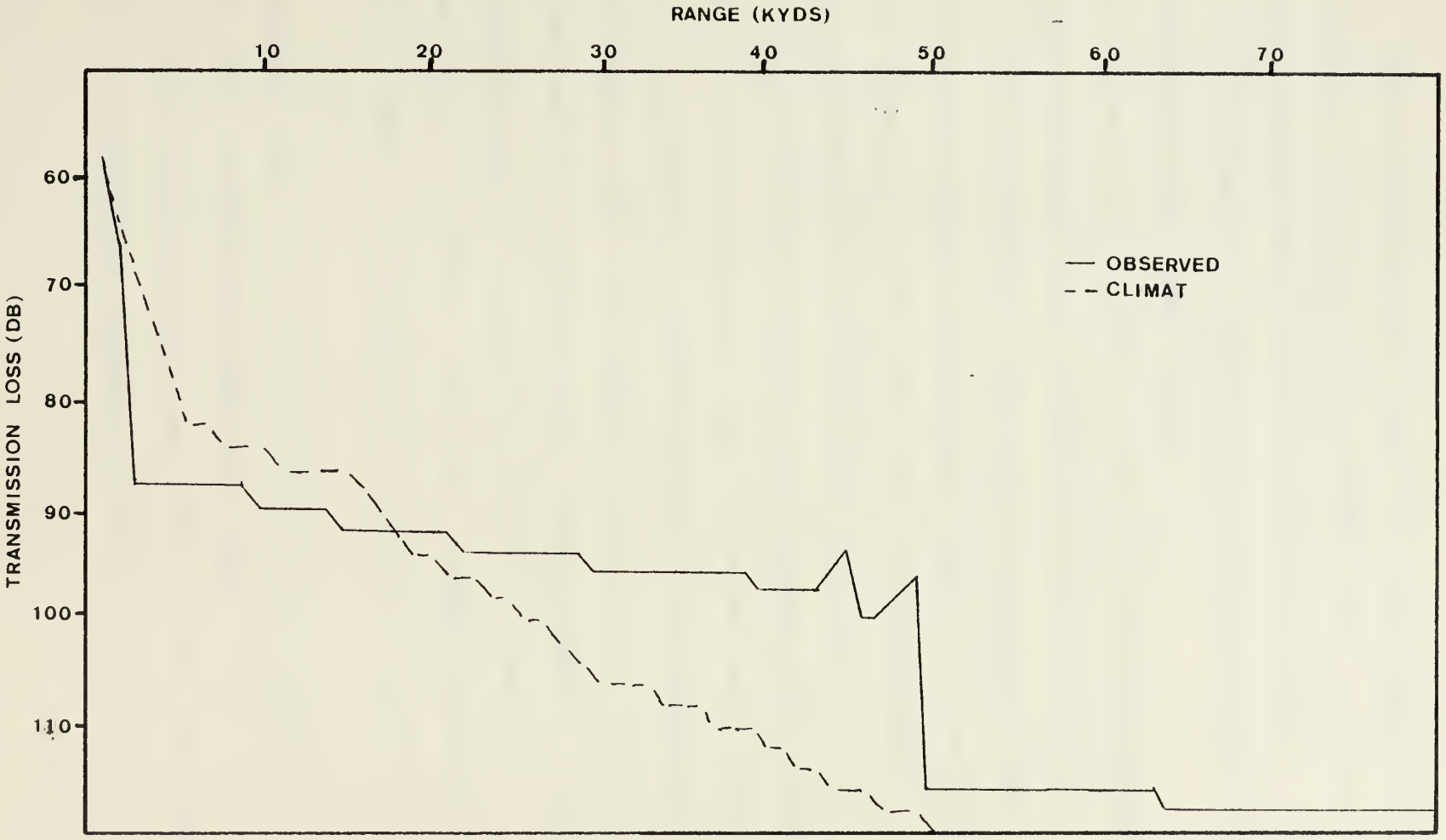

Figure 37. Transmission loss curves for Station 10.
Source at 100 m, receiver at 10 m, 2000 Hz.

As a towed array nears the edge of an eddy, prediction by ICAPS historical data improves for higher FOM's. At low FOM's (< 90 dB) the accuracy of the prediction was poor. CZ propagation was successfully predicted by historical data and should be expected in the Somali Basin.

Poor ranges were expected in the cold upwelling areas. However, ranges predicted from the observed data were much greater than within the eddies. The areas of upwelling are extensive and ranges can be realistically expected to be great. Channeling is present to some degree in all observed SSP's. Climatological predictions were generally accurate.

A higher frequency (2000 Hz) hull mounted sonar located in the body of the main warm core eddy can expect much greater range than that predicted by ICAPS because of the presence of the strong surface layer. The observed range in this eddy is twice as great as that observed in the smaller eddies. Climatological predictions in the smaller eddies are generally accurate but ranges are short (less than 13 kyds) at FOM's of 80 and 90 dB. Ranges are significantly greater at an FOM of 100 dB.

Near the eddy's edge, hull mounted sonar ranges are short (less than 10 kyds for an FOM of 80 and 90 dB). The accuracy of ICAPS climatological prediction is good with actual differences in observed and historical predictions of less than 2 kyds.

High frequency sonars operating in the cold upwelling areas can expect good accuracy from the climatological range predictions at FOM's greater than 80 dB. Ranges are generally longer in these areas except at an FOM of 80 dB where ranges are shorter than in other areas.

The climatology does not accurately represent the physical characteristics of the area in that it does not reflect the eddy field. The absence of the strong main eddy leads to a serious underestimation of detection ability. Despite the fact that the climatology does not reflect the complex thermal structure of the western Indian Ocean during the summer season, predictions based on climatology are accurate enough for operational use.

The use of a single sound speed profile for the 200 kyd range of ICAPS during the summer season appears to be valid because of the large size of the features.

2. Winter Monsoon

During the winter season climatological predictions were extremely poor despite the absence of a complicated thermal field such as exists during the summer. A towed array would experience below layer transmissions and ranges significantly longer (2 to 3 times greater) than those predicted by the ICAPS climatology primarily due to the intense channeling found in the upper 1000 m of the observed SSP's. Ranges can be expected to be great, e.g., 70 kyds at FOM of 90 dB and 159 kyds at an FOM of 100 dB.

Hull mounted sonars can expect *in situ* ranges less than 13 kyds for FOM's less than 90 dB. The ICAPS climatology greatly overpredicted ranges at these FOM's by an average of 84% because of a less severe gradient in the upper thermocline. At an FOM of 100 dB, the inverse was true with the climatological data inaccurately underpredicting the range by an average of 46%. This occurred because the TL curve for the observed data leveled out at approximately 90 dB while the climatological TL curve continued to fall off.

Climatological SSP's did not reveal the complexity of those observed. The strong influence of the warm, saline RSIW and PGIW was observed in the upper 1000 m where intense ducting occurred. Climatological data revealed no ducting at all.

The range independence of the ICAPS program is extremely compromising during the winter season because of the great variability observed in SSP's.

In winter, the ICAPS climatology does not adequately reflect the observed complex water mass structure which causes great variability in the sound speed structure. Median detection range accuracy based on historical temperature-salinity data is so poor as to be useless in operational planning.

IV. CONCLUSIONS

When planning and conducting ASW operations utilizing surface platforms in the Somali Basin, one can expect:

1. ICAPS predictions of direct path detection range based on climatology to be extremely inaccurate during the winter monsoon. At 100 Hz ICAPS range predictions based on climatology were short by a factor of about two due to intense channeling observed in the upper 1000 m and not indicated in the historical SSP. At 2000 Hz ICAPS caused an overprediction of detection range at FOM's less than 90 dB because of less severe gradients in the upper thermocline. At higher FOM's ICAPS underpredicted performance by a factor of about two, again because of the intense channeling in the in situ data;

2. ICAPS predictions of direct path detection range based on climatology are generally accurate during the summer monsoon except within the "prime" warm core eddy;

3. Within the "prime" eddy in situ ranges are two to three times greater than estimated by forecasts based on climatology because of the existence of the deep surface duct not present in the climatology; and,

4. Within the western Indian Ocean convergence zone propagation is possible only within deep waters of the Somali Basin. Sufficient depth excess exists throughout the year except in March where previous studies have shown CZ propagation

to be either absent or only slightly possible. This study showed that CZ propagation could be expected at all stations having bottom depths deeper than 4500 m.

BIBLIOGRAPHY

Bruce, J.G., (1979). "Eddies off the Somali Coast during the Southwest Monsoon." J. Geophys. Res., 84 (c12), p. 7742-7748.

Cadet, D., (1979). "Meteorology of the Indian summer monsoon." Nature 279, p. 761-767.

Colborn, J.G., (1976). "Sound speed distribution in the western Indian Ocean." NUC TP 502.

Düing, W., (1980). "Somali Current: evolution of surface current." (In Press).

Fairbridge, R.W., (1966). Encyclopedia of Oceanography. New York: Reinhold.

Fenner, D.F., and W.J. Cronin, (1978). Bearing Stake Exercise: sound speed and other environmental variability. NORDA, NSTL Station, Miss. Report #18.

Knox, R., (1980). Indian Ocean Primer. Unpublished manuscript. Scripps Institution of Oceanography, La Jolla, CA.

Leetmaa, A., (1972). "The response of the Somali Current to the southwest monsoon of 1970." Deep-Sea Res., 19, p. 319-326.

_____. (1973). "The response of the Somali Current at 2°S to the southwest monsoon of 1971." Deep-Sea Res., 20(4), p. 397-400.

_____. (1980). "Somali Current: subsurface circulation." (In Press).

Luyten, J.R., and J.C. Swallow, (1976). "Equatorial undercurrents." Deep-Sea Res., 23, p. 999-1001.

Neumann, G. and W.J. Pierson, (1966). Principles of Physical Oceanography. Englewood Cliffs: Prentice Hall.

Pickard, G.L., (1975). Descriptive Physical Oceanography. New York: Pergamon Press.

Shepard, F.P., (1973). Submarine Geology. New York: Harper and Row.

Sverdrup, H.U., M.W. Johnson, and R.H. Fleming, (1942). The Oceans. Englewood Cliffs: Prentice Hall.

Swallow, J.G. and J.G. Bruce, (1966). "Current measurements off the Somali coast during the southwest monsoon of 1964." Deep-Sea Res., 13, p. 861-888.

Warren, B., H. Stommel, and J.C. Swallow, (1966). "Water masses and patterns of flow in the Somali Basin during the southwest monsoon of 1964." Deep-Sea Res., 13, p. 825-860.

Wyrtki, K., (1971). Oceanographic Atlas of the International Indian Ocean Expedition. Washington, D.C.: National Science Foundation,

SP-68 (1966). Handbook of Oceanographic Tables. U.S. Government Printing Office.

HO-107 (1971). Atlas of Pilot Charts of South Pacific and Indian Oceans. Defense Mapping Agency.

INITIAL DISTRIBUTION LIST

		No. Copies
1.	Defense Technical Information Center Cameron Station Alexandria, Virginia 22314	2
2.	Library, Code 0142 Naval Postgraduate School Monterey, California 93940	2
3.	Department Chairman, Code 68 Department of Oceanography Naval Postgraduate School Monterey, California 93940	1
4.	Assoc. Professor R.H. Bourke, Code 68 Bf Department of Oceanography Naval Postgraduate School Monterey, California 93940	1
5.	LT J.S. Hanna, USN Rt. 4, Box 92b Dover, Delaware 19901	1
6.	Mr. William Beatty CDR/U.S. Naval Oceanographic Office NSTL Station Bay St. Louis, Mississippi 39522	1
7.	Director Naval Oceanography Division Navy Observatory 34th and Massachusetts Avenue NW Washington, D.C. 20390	1
8.	Commander Naval Oceanography Command NSTL Station Bay St. Louis, Mississippi 39529	1
9.	Commanding Officer Naval Oceanographic Office NSTL Station Bay St. Louis, Mississippi 39529	1

10. Commanding Officer — 1
Fleet Numerical Oceanography Center
Monterey, California 93940

11. Commanding Officer — 1
Naval Ocean Research & Development Activity
NSTL Station
Bay St. Louis, Mississippi 39529

12. Office of Naval Research (Code 480) — 1
Naval Ocean Research & Development Activity
NSTL Station
Bay St. Louis, Mississippi 39529

13. Scientific Liaison Office — 1
Office of Naval Research
Scripps Institution of Oceanography
La Jolla, California 93037

14. Commanding Officer — 1
Naval Oceanography Command Center, Guam
Box 12
FPO San Francisco 96630

Thesis
H1967
c.1
192578
Hanna
Acoustic propagation
in the Somali basin.